Anomalies of Dorsal Induction: Neural Tube Defects

6

Dorsal induction refers to the development of the neural tube as a result of induction by the notochord. The notochord develops during the third week of conceptual age along the cephalocaudal axis of the trilaminar embryo. It induces the neural plate (neurectoderm) to form the neural groove. The neural groove closes to form the neural tube between the 22nd and 26th day of conceptual age. The rostral and caudal neuropores close by the 24th and 26th days of conceptual age, respectively. The process of dorsal induction is also referred to as primary neurulation. The neural tube gives rise to the brain and spinal cord. Total or partial failure of closure of the neural groove results in neural tube defects (defects of dorsal induction).

These include:

Failure to closure	Defect
Rostral neuropore	Anencephaly
Caudal neuropore	Sacral spina bifida
Calvarium	Encephalocele
Segmental failure	Open Spina bifida
Entire neural tube	Craniorachischisis

The neural development caudal to the caudal neuropore is termed secondary neurulation. Secondary neurulation follows primary neurulation and occurs at 5–6 weeks conceptual age. The conus medullaris, filum terminale and the spine caudal to the midsacral region develop by secondary neurulation. Due to differential growth between the vertebral column and spinal cord, the conus medullaris moves rostrally. Closed spina bifida with lipomatous lesions is the result of defective secondary neurulation.

6.1 Anencephaly

Exencephaly or acrania is the absence of the calvarium. Early, during 11–14 weeks gestational age, a fairly well-formed brain, without the calvarium, is seen. The embryonic brain is exposed to amniotic fluid resulting in its disintegration. Total disintegration of the brain results in anencephaly.

The ultrasound findings are as follows:

1. The base of the skull and face is seen.
2. The brain is not confined by the presence of the echogenic calvarium, and hence it appears broad and bilobed. Lateral ventricles and choroid plexus may be seen. As disintegration sets in, there may be cystic spaces in the brain. Absence of calvarial bones can be recognised as early as 10–11 weeks.
3. By the second and third trimesters, the classical anencephaly appearance is seen (Fig. 6.1). The calvarium above the level of the orbits and brain is not seen. There could be loose, spongy, floating, echogenic glial tissue (area cerebrovasculosa) in the defect.
4. The orbits are present and appear prominent giving rise to the 'frog facies' on the coronal sections. The severity of the malformation enables easy detection especially in the second and third trimesters.
5. In about 50% of the cases, there is polyhydramnios.
6. Anencephaly due to amniotic band syndrome may be suspected if there is asymmetric absence of calvarial bones. Other features of disruption like digit amputation or anterior abdominal wall defects may be seen. Demonstration of amniotic bands connecting the defect to the placenta or uterine wall confirms the diagnosis. This is a nonrecurring cause of anencephaly (Fig. 6.2).

Anencephaly is multifactorial and is causally related to low maternal serum folic acid levels. Periconceptional folic acid therapy prevents recurrence. Mutations in the MTHFR gene are associated with an increased risk of open spina bifida. Anencephaly can also be due to chromosomal abnormality (Tri 13, 18 or 21), syndrome (Meckel-Gruber syndrome) or teratogenicity (valproic acid or carbamazepine).

B. S. Rama Murthy, *Imaging of Fetal Brain and Spine*, https://doi.org/10.1007/978-981-13-5844-9_6

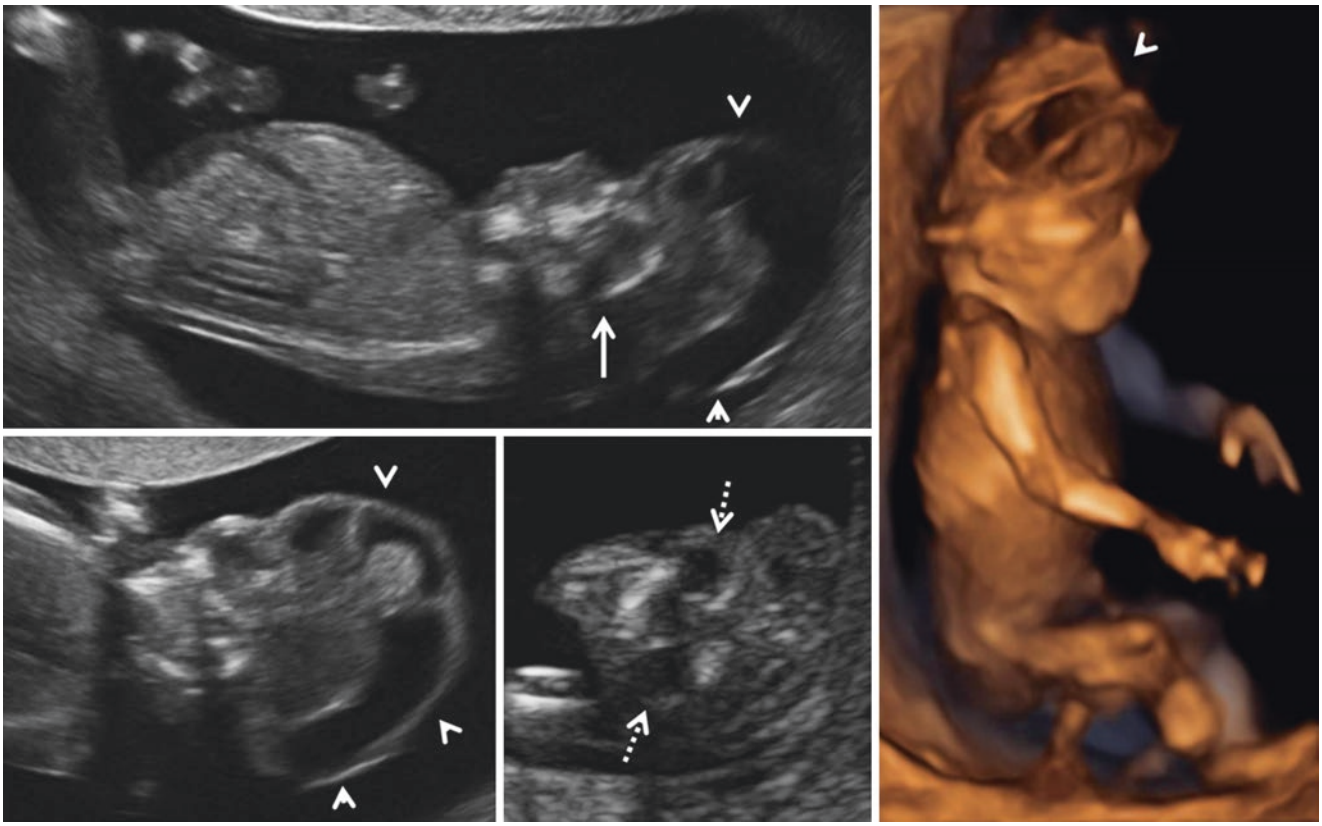

Fig. 6.1 15 weeks (TVS) *anencephaly* – sagittal sections of the fetus and cranial region, coronal section of the cranial region and 3D surface rendering of the fetus – absent calvarial bones, base of skull (solid arrow), loose spongy neuroglial tissue (arrowheads), orbits (dotted arrows)

Higher incidence of anencephaly is seen with maternal diabetes. Associated abnormalities may include varying degrees of open spina bifida, congenital heart defects, esophageal or jejunal atresia, hydronephrosis, facial clefting and abdominal wall defects.

6.2 Iniencephaly

This is a lethal neural tube defect characterised by an occipital bony defect, failure of closure of the cervicothoracic segments and absent or short extended neck, with an upward-turned face.

The ultrasound findings are as follows:

1. Upward-tilted face due to persistent neck extension.
2. The spine is short and lordotic with cervical and upper thoracic vertebral defects (Fig. 6.3).
3. Occipital encephalocele (protruding through the foramen magna) may be seen.
4. The neck is absent. The anterior chest wall is directly continuous with the chin.
5. Associated defects include anencephaly, microcephaly, hydrocephalus, open spina bifida and facial clefts.

Differential diagnosis is Klippel-Feil syndrome in which a short neck is present with cervical spine anomalies such as block vertebra.

6.3 Cephalocele

Herniation of intracranial structures through a calvarial bony defect is termed a cephalocele. Depending on the herniated structures, a cephalocele may be a meningocele, encephalocele or encephalocystocele. Herniation of meninges alone is termed meningocele. Herniation of meninges and a part of the occipital lobe/s is termed an encephalocele. If a part of the ventricle herniates with the brain, the term encephalocystocele is used. Depending on the site of the calvarial defect, an encephalocele could be occipital, frontal, temporal or parietal. The occipital and frontal lesions are embryologic defects. They are generally covered with skin. Parietal lesions are non-embryologic and are due to amniotic band disruption. Ninety percent of encephaloceles are occipital.

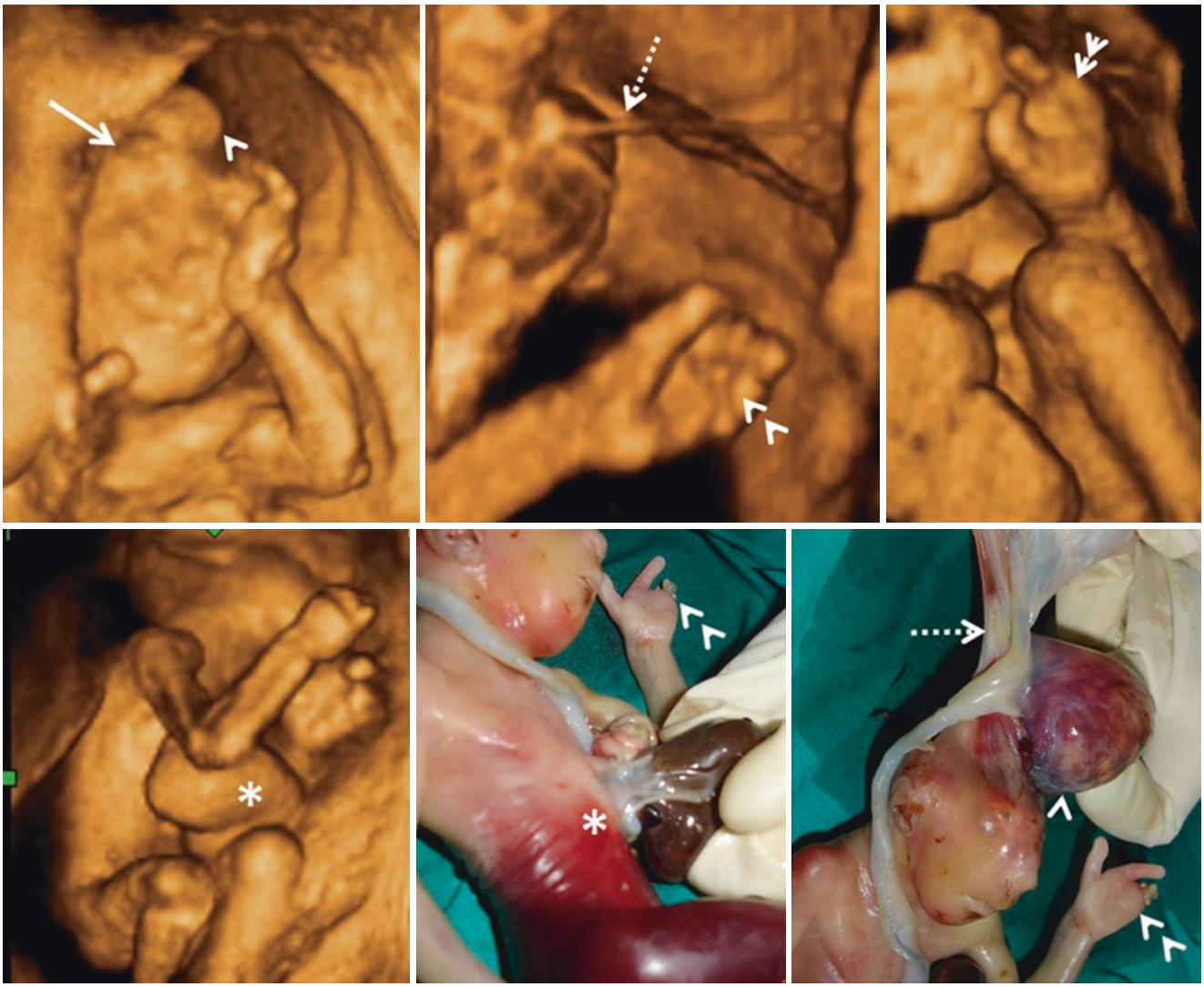

Fig. 6.2 19 weeks (TAS 3D US) *acrania/exencephaly due to amniotic band sequence* – 3D surface-rendered views of the head and face, left hand and trunk of the fetus – absent calvarial bones, base of skull (solid arrow), residual brain (arrowhead), amniotic bands attached to the base of skull (dotted arrow), digit amputation (double arrowheads), gastroschisis (*)

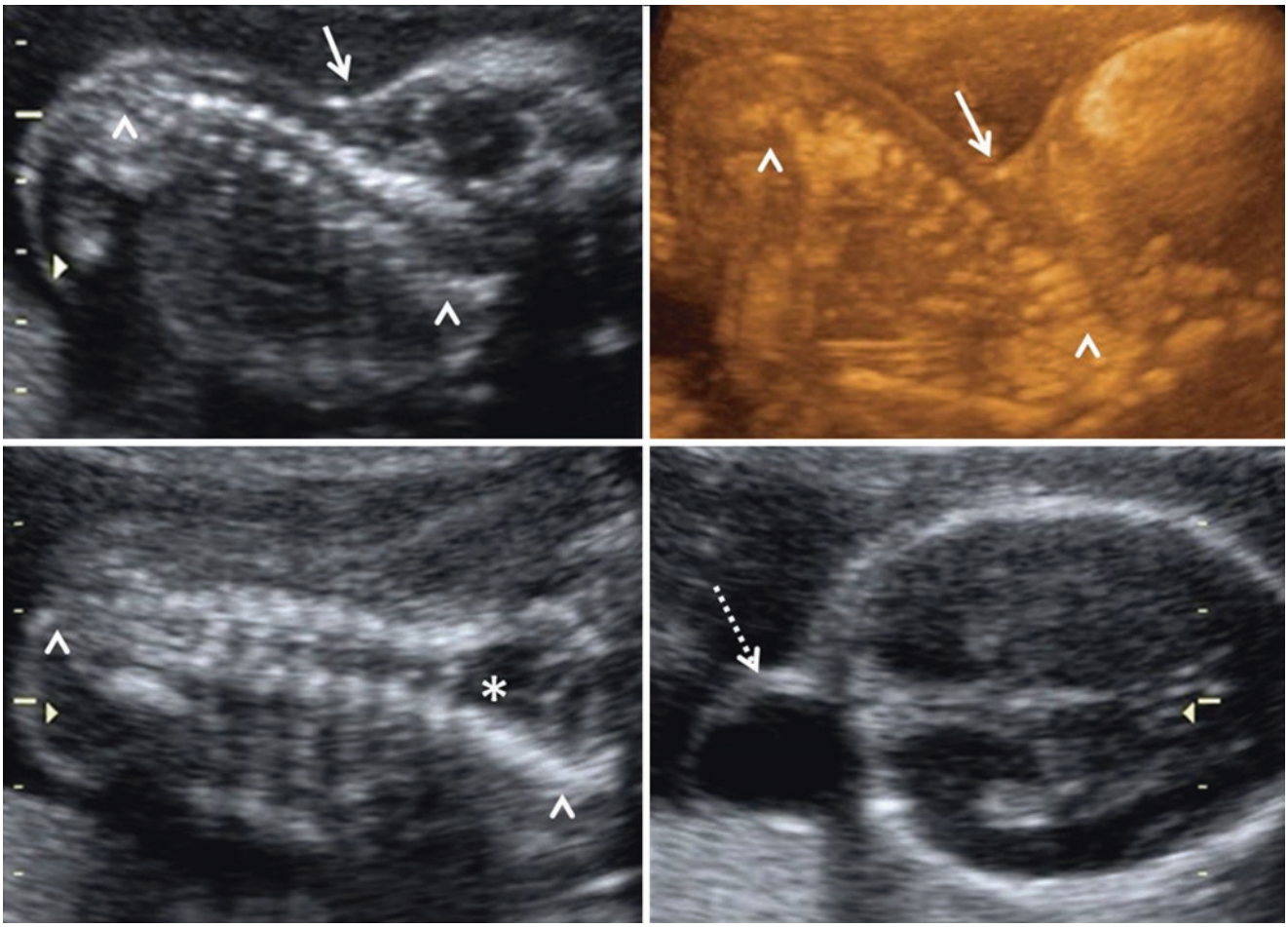

Fig. 6.3 19 weeks (TAS) *iniencephaly* – sagittal section of spine and cranium, 3D rendered image of spine in maximum mode, coronal section of spine, axial transventricular section of cranium – short length of spine (arrowheads), extension at the craniovertebral junction (solid arrow), splaying of the posterior ossific centres in the cervical spine (*), occipital meningocele (dotted arrow)

6.3.1 Occipital Cephalocele

The ultrasound findings are as follows:

1. Encephalocele is seen as a thin-walled sac containing the occipital lobe or lobes, adjacent to the calvarial defect. The size of the lesion may vary from a very small sac of few millimetres to a sac larger than the cranium. The posterior horn is herniated with the occipital lobe/s in encephalocystocele (Figs. 6.4, 6.5 and 6.6).
2. Herniation of the meninges alone results in a thin-walled, subcutaneous, cystic occipital meningocele (Fig. 6.7). This lesion is filled with CSF.
3. Bony calvarial defect of variable size can be identified. 3D rendering with maximum mode in the coronal plane can display the calvarial defect to advantage.
4. The communication between the intracranium and the sac can be traced.
5. Obstructive hydrocephalus may be seen (Fig. 6.6).
6. In low occipital and high cervical defects, the cerebellum may herniate across the foramen magnum and present as an encephalocele at the craniovertebral junction. This is termed Chiari III malformation (Fig. 6.8).
7. If a sizable volume of the brain has herniated, there is consequent microcephaly (Fig. 6.4).

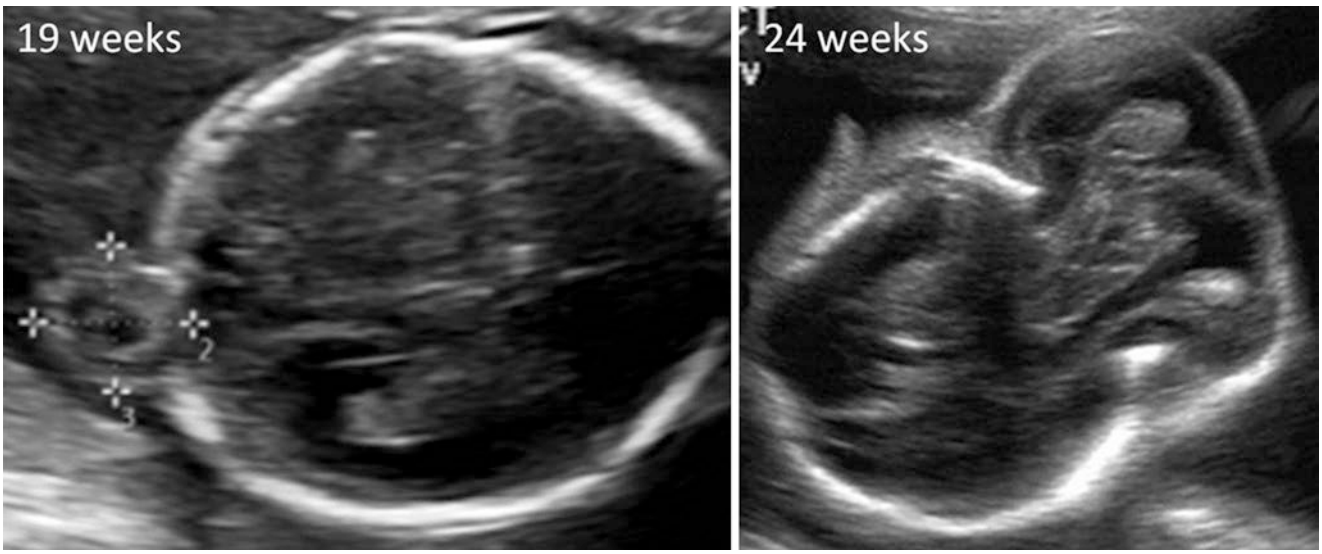

Fig. 6.4 Two cases, one at 19 and the other at 24 weeks (TAS) *small occipital encephalocele, large occipital encephalocystocele* – axial sections – the bony defect and lesion are larger in size in the latter compared to the former. Herniation of a larger volume of brain has resulted in a smaller size of the cranium in the latter

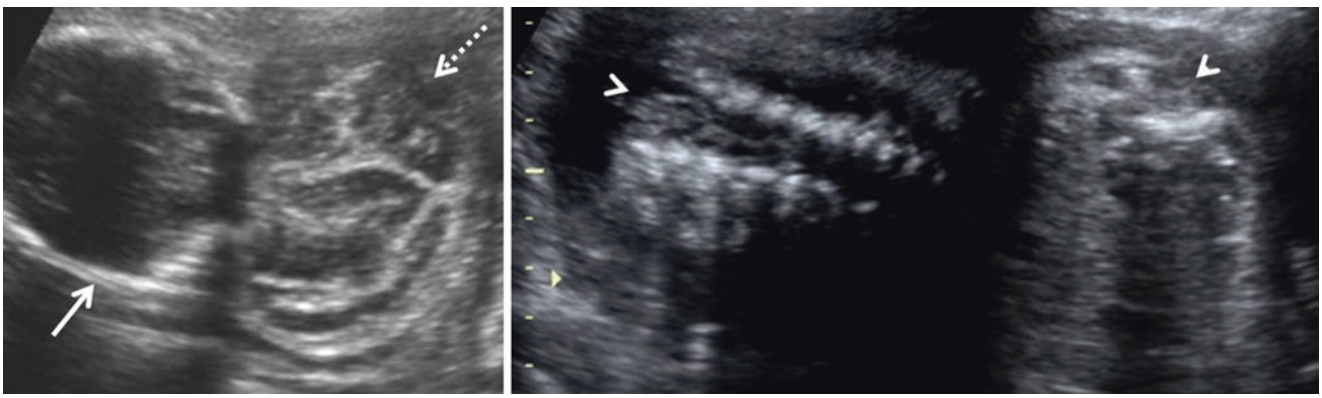

Fig. 6.5 24 weeks (TAS) *occipital encephalocystocele and thoracolumbar open spina bifida* – axial section of cranium, coronal and axial sections of the fetal lumbar spine – large occipital encephalocele (dotted arrow), consequent microcephaly (solid arrow), splaying of posterior ossific centres of the thoracolumbar spine (arrowheads)

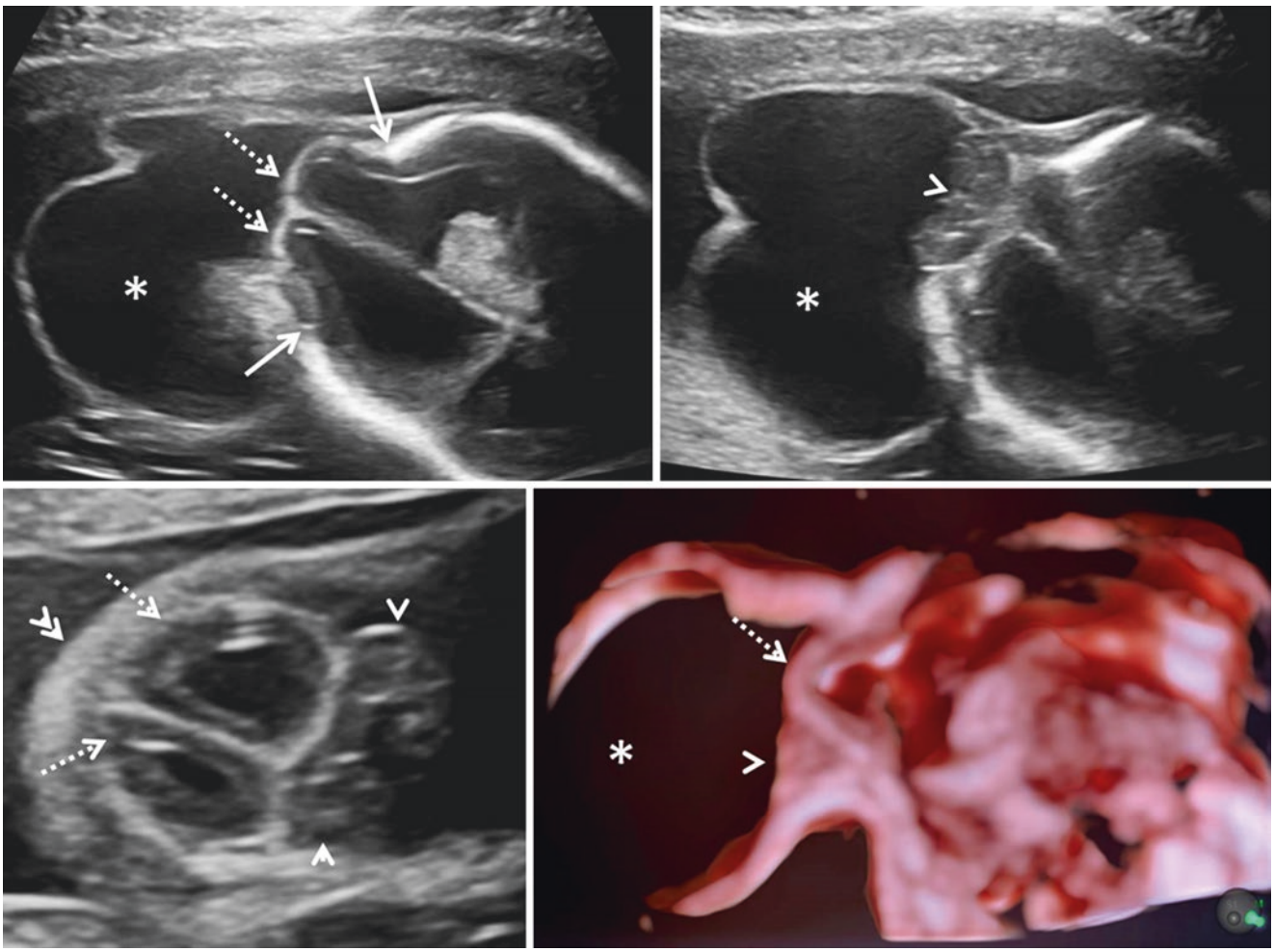

Fig. 6.6 20 weeks (TAS linear 9 MHz) *occipital encephalocystocele* – axial sections at slightly cephalad and caudad planes, coronal section and 3D rendered parasagittal section – margins of large occipital bony defect (solid arrows), occipital lobes and posterior horns on both sides (dotted arrows) and entire cerebellum (arrowhead) have herniated into the lesion, a major portion of the lesion is filled with fluid (*), skin is covering the encephalocystocele (double arrowhead)

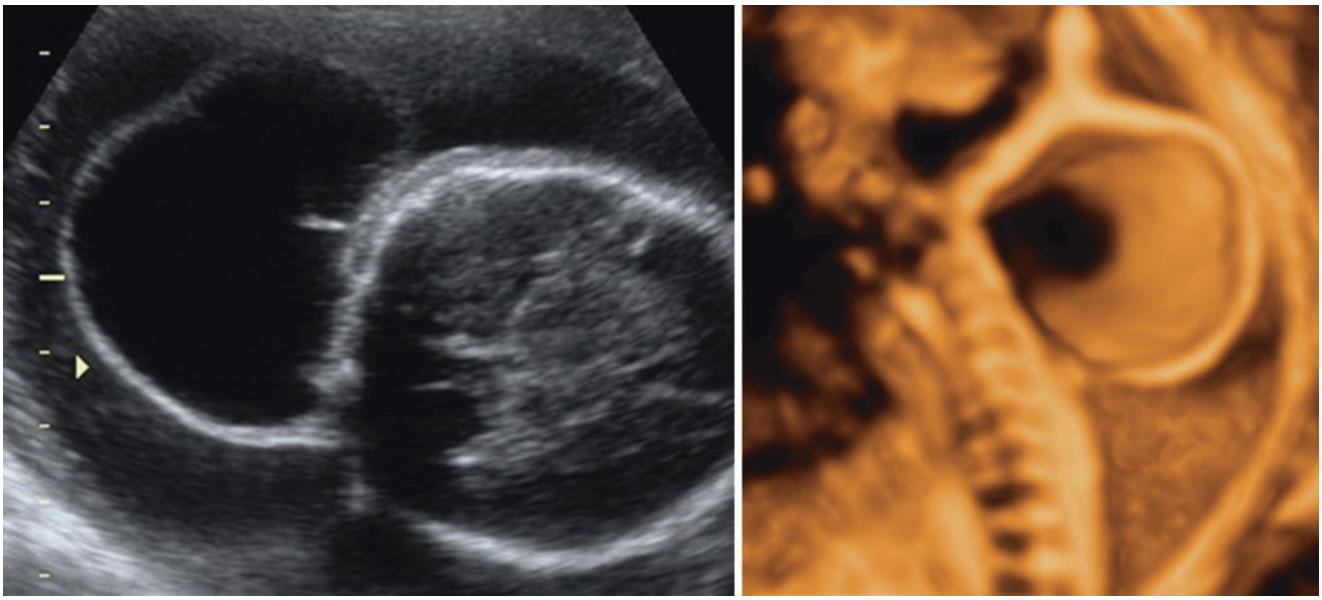

Fig. 6.7 23 weeks (TAS) *occipitocervical meningocele* – axial transventricular section, 3D rendered image of the craniovertebral region – meningocele (solid arrow), no evidence of herniated brain

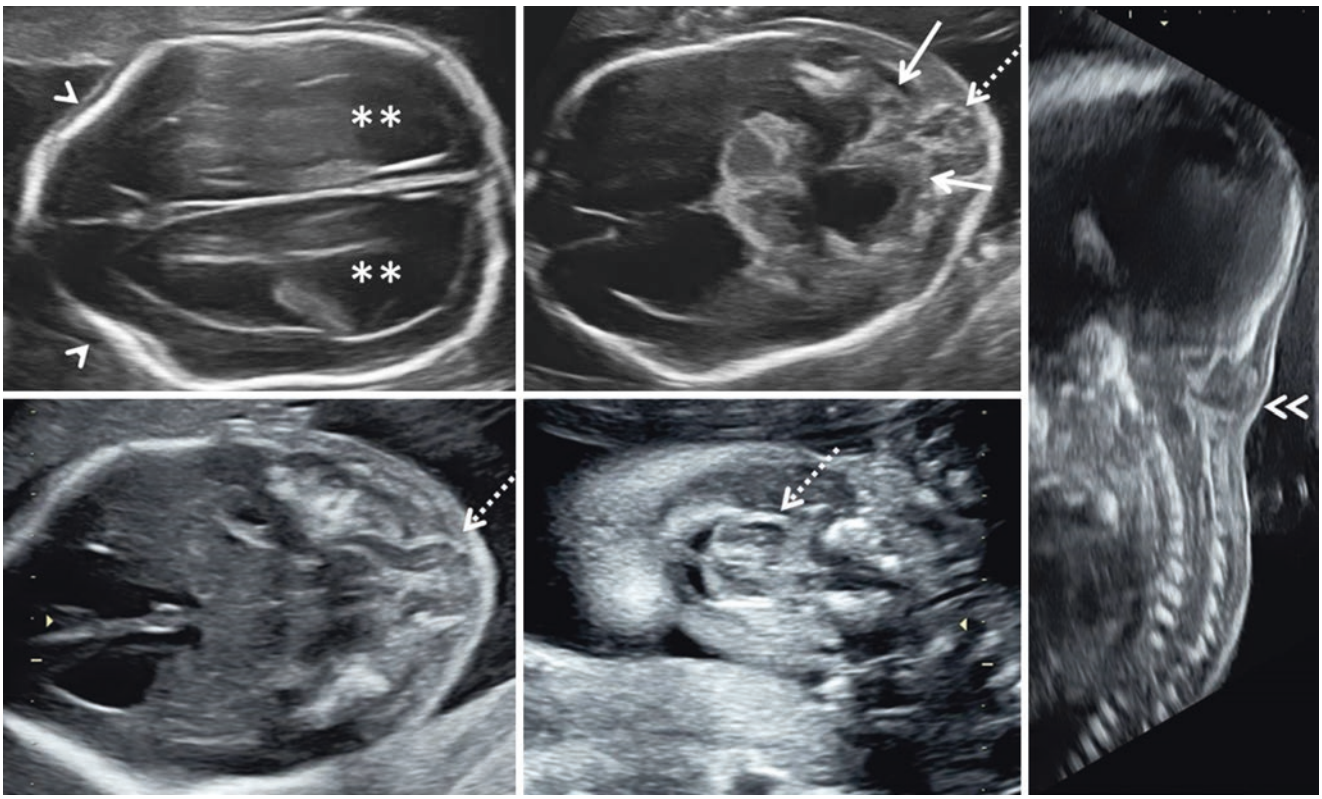

Fig. 6.8 20 weeks (TAS) *Chiari III malformation* – axial transventricular and transcerebellar sections, coronal and midsagittal sections – bilateral lateral ventriculomegaly (**), 'lemon' sign (arrowheads), occipital lobes are intracranial (solid arrows), herniation of the entire cerebellum into an occipitocervical encephalocele (dotted arrows), the skin cover over the encephalocele is intact (double arrowhead). Mid thoracic hemivertebra and lumbar spina bifida were also noted in this fetus

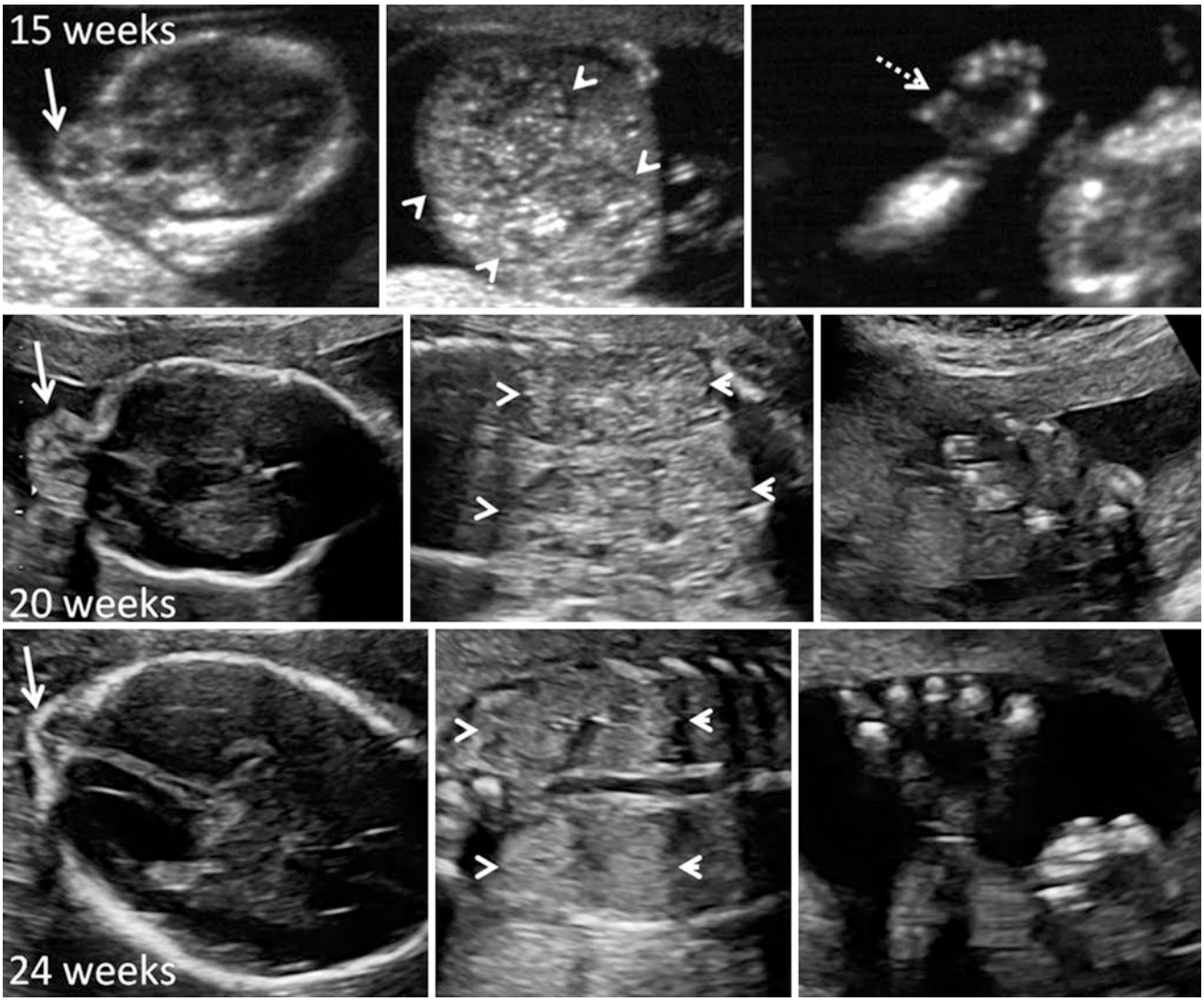

Fig. 6.9 Three different cases of *Meckel-Gruber syndrome* at 15, 20 and 24 weeks (TAS) – axial transventricular cranial sections, axial or coronal abdominal sections, coronal sections of the fetal hand – occipital encephalocele (solid arrows), enlarged hyperechoic kidneys with small macrocysts (arrowheads), postaxial polydactyly seen only in the first case. History of 3° consanguinity was present in the third case

Occipital encephalocele may be syndromic or nonsyndromic (multifactorial). Associated anomalies occur in about 65% of nonsyndromic encephaloceles. These include congenital heart defects, pelviectasia, renal agenesis, talipes, diaphragmatic hernia and anterior abdominal wall defects. Fetal karyotyping is indicated as there is a 14–18% risk of chromosomal abnormality.

Two autosomal recessive syndromes that are associated with occipital encephalocele are Meckel-Gruber and Walker-Warburg syndromes.

About 80% of cases of Meckel-Gruber syndrome (lethal) have occipital encephalocele. The other major findings are enlarged cystic kidneys, postaxial polydactyly and facial clefting. Anhydramnios due to the lack of fetal renal function is seen in the second trimester with consequent Potter sequence. Dandy-Walker malformation, congenital heart defects and microphthalmia may also be associated with Meckel-Gruber syndrome (Fig. 6.9).

Walker-Warburg syndrome is also known as HARD+/-E syndrome. This is an acronym for hydrocephalus, agyria and retinal dysplasia with or without encephalocele. Encephalocele is seen in 26% of cases. Associated Dandy-Walker malformation may be noted. This is discussed in the chapter on malformations of cortical development.

Occipital encephalocele should be differentiated from a cystic hygroma. The absence of calvarial defect, normal intracranium and presence of septation are diagnostic of cystic hygroma. Other differential diagnoses include sebaceous cyst, teratoma and haemangioma.

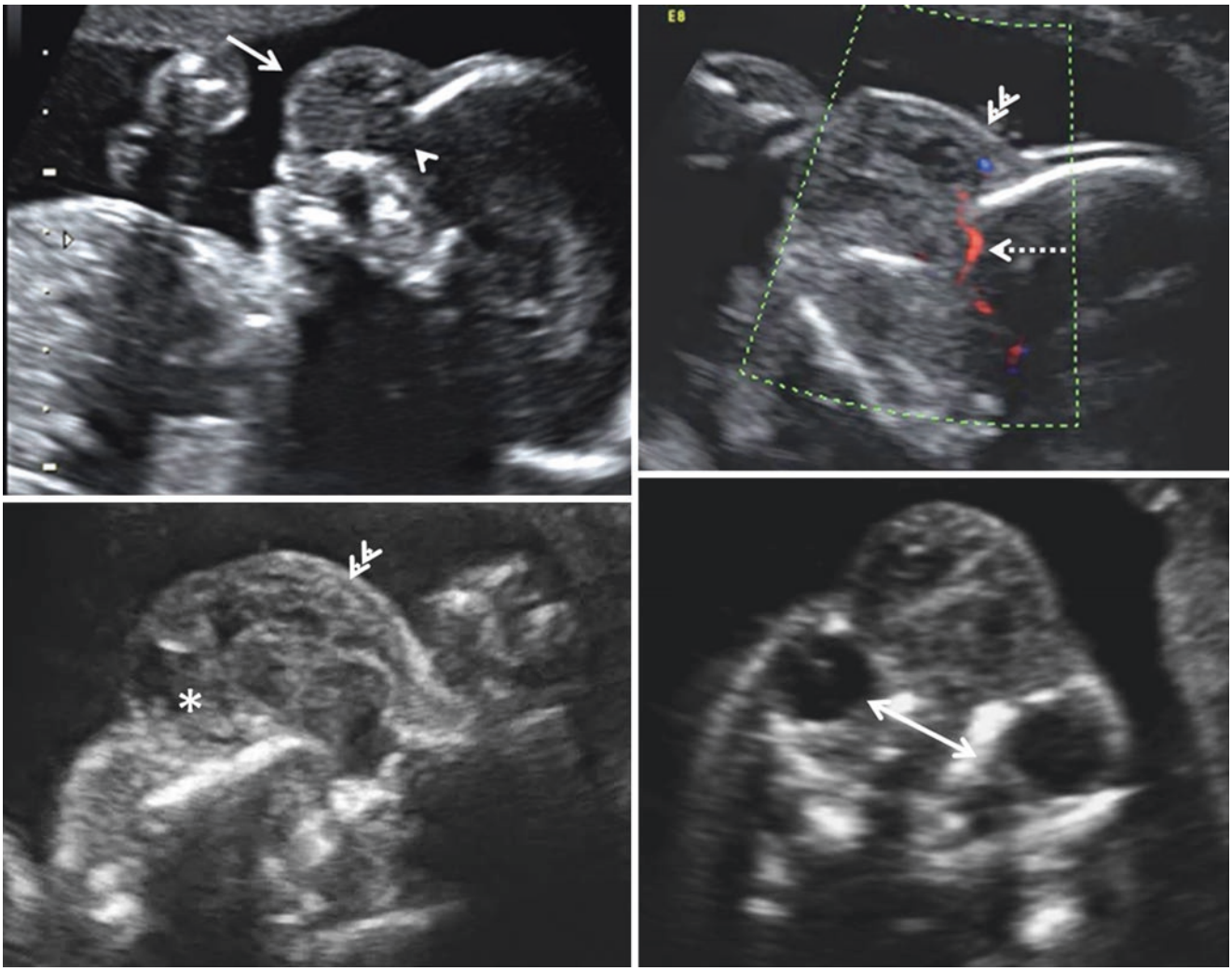

Fig. 6.10 20 weeks (TAS) *frontal encephalocele* – midsagittal sections of fetal face B mode and color Doppler, magnified axial section of the lesion, axial section of the orbits – defect in the frontal bone (arrowhead), overlying soft tissue mass (solid arrow), intracranial artery coursing through bony defect into the lesion (dotted arrow), brain echoes seen in the lesion (*), hypertelorism (double-headed arrow). Note the presence of skin covering the encephalocele (double arrowheads)

6.3.2 Frontal Cephalocele

The ultrasound findings are as follows:

1. The lesion is located in the frontal and interorbital regions (Fig. 6.10).
2. Hypertelorism is present.
3. A cystic lesion with or without herniated brain tissue is seen.
4. The calvarial defect can be visualised.
5. Hypertelorism, bifid nose and median cleft lip are findings with frontal encephalocele in frontonasal dysplasia (Fig. 6.11a, b).
6. Callosal agenesis and hydrocephalus may be associated with frontal encephalocele.

Differential diagnosis includes dermal sinus cyst, haemangioma and teratoma.

6.3.3 Parietal Cephalocele

Parietal encephalocele is a non-embryologic defect and is located off the midline. Focal calvarial disruption by amniotic bands results in herniation of the meninges and brain tissue. Other features of amniotic band disruption are amputation of digits, gastroschisis and bizarre facial clefting. Visualisation of amniotic bands adherent to the cranium confirms the diagnosis. As amniotic band sequence is sporadic, the risk of recurrence does not increase in subsequent pregnancies (Fig. 6.12).

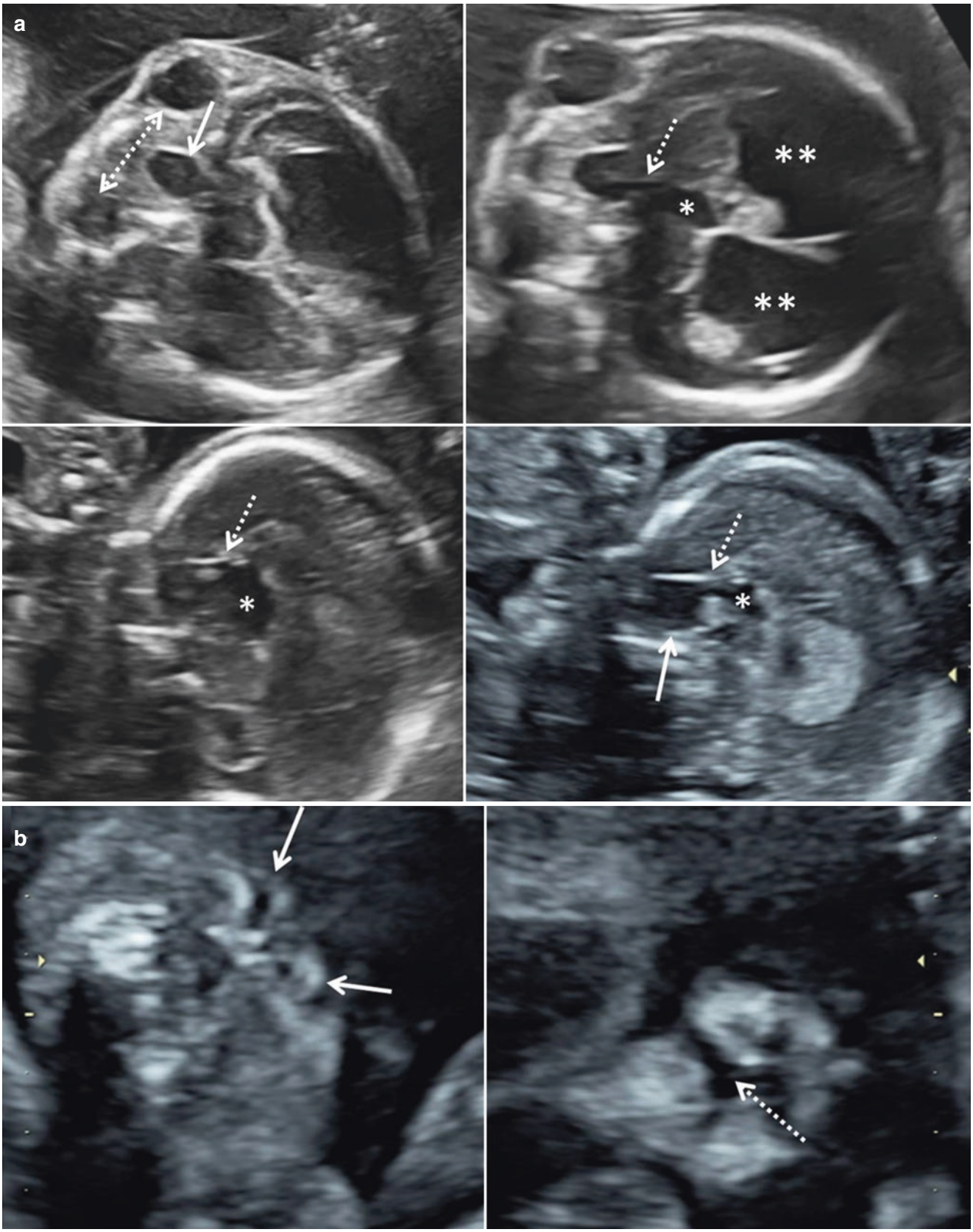

Fig. 6.11 (**a**) 20 weeks (TAS) *fronto-ethmoidal meningocele in frontonasal dysplasia fetus A of a monochorionic diamniotic pair* – axial sections of the orbits, midsagittal sections of the cranium – hypertelorism (double-headed arrow), interorbital ovoid cystic lesion (solid arrow), communicating with the third ventricle posteriorly (dotted arrow), bilateral lateral ventriculomegaly (**) and third ventriculomegaly (*). (**b**) 20 weeks (TAS) *fronto-ethmoidal meningocele in frontonasal dysplasia in fetus A of a monochorionic diamniotic pair* – semicoronal and coronal sections of the nose and lips, midsagittal section of the face – the two nostrils are separated (solid arrows) indicating bifid nose, median cleft lip (dotted arrow), flat nasal profile (arrowhead)

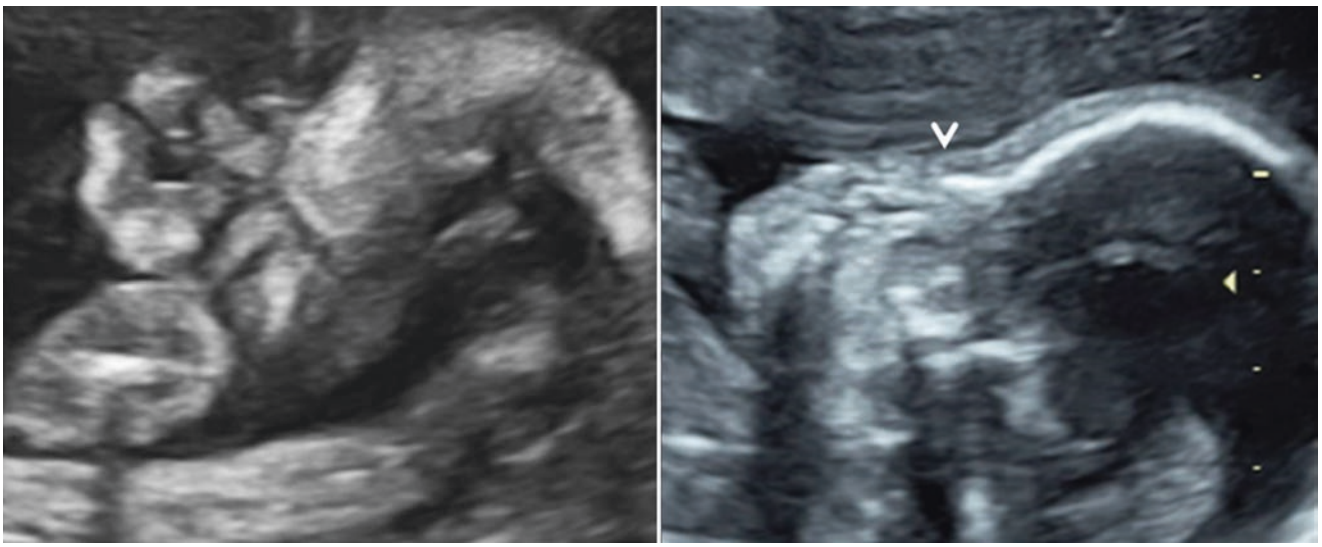

Fig. 6.11 (continued)

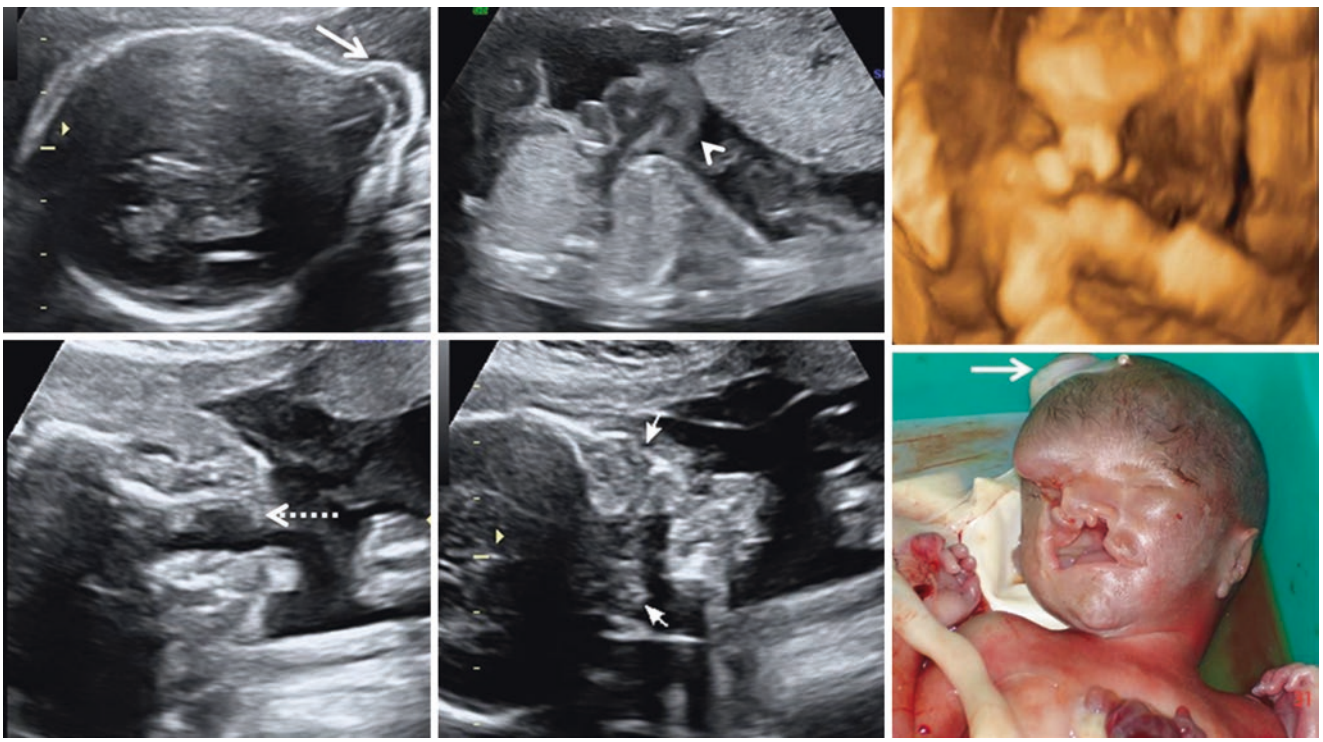

Fig. 6.12 23 weeks (TAS) *right parietal encephalocele due to amniotic band sequence* – axial transventricular section, axial section of thorax, 3D surface rendering of fetal face, axial section of the upper lip and jaw, axial section of orbits, picture of the abortus – parietal encephalocele (solid arrow), ectopia cordis (arrowhead), cleft of the lip and palate (dotted arrow), bilateral microphthalmia (small arrows)

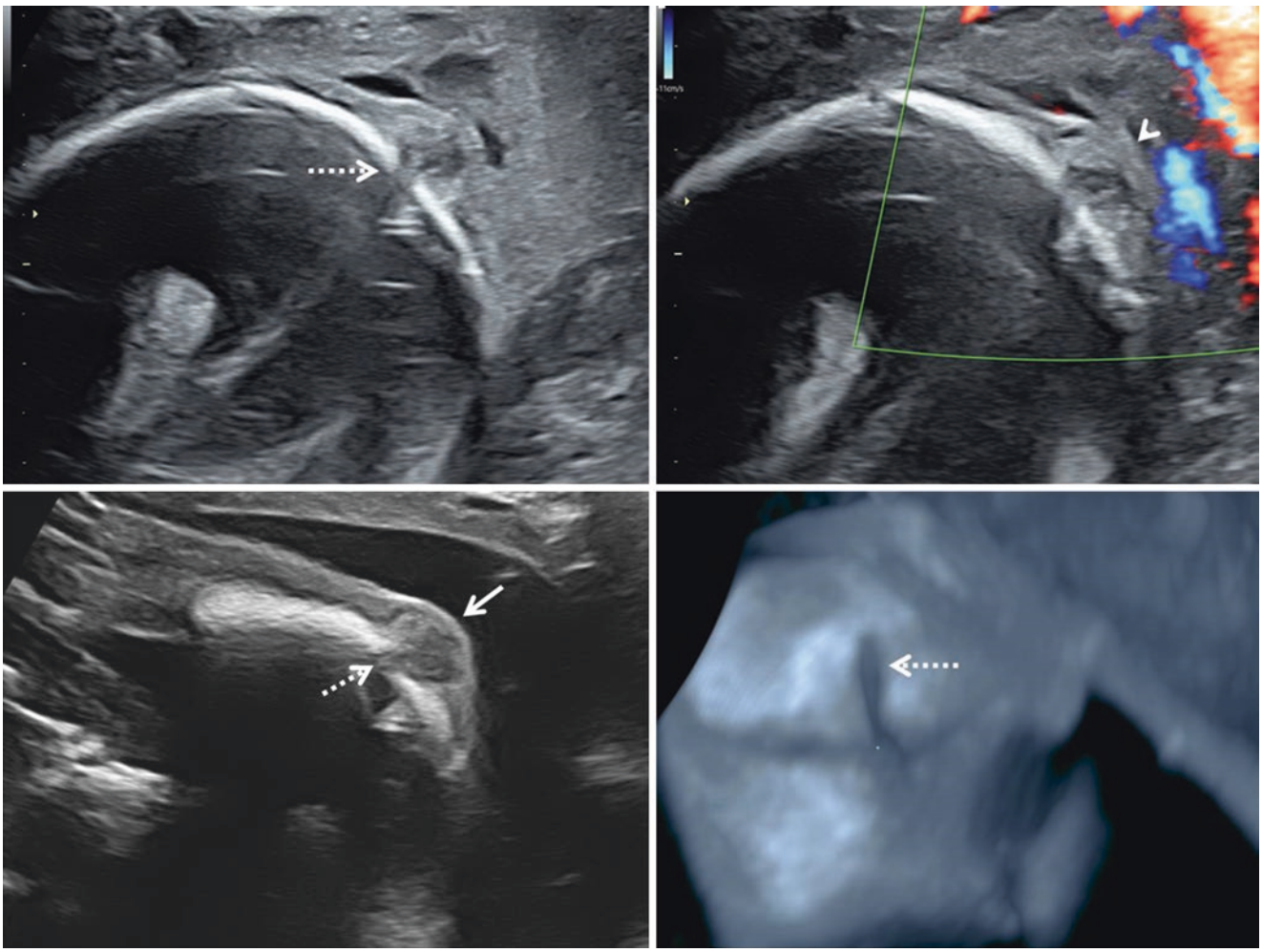

Fig. 6.13 22 weeks (TAS) *atretic cephalocele* – axial transventricular section B mode and color Doppler, magnified sagittal section, 3D thick slice volume contrast imaging of the occipital bone – atretic cephalocele over the occipital bone (solid arrow), bony defect underlying the cephalocele (dotted arrows), no color Doppler signal in the cephalocele (arrowhead). Note the skin covering the cephalocele. Associated findings of Blake's pouch cyst and unilateral pelviureteric junction obstruction were present

6.3.4 Atretic Cephalocele

This lesion presents as a small midline scalp swelling in the region of the posterior fontanelle. An atretic cephalocele is composed of subgaleal fibrous tissue with elements of meninges and neuroglia. It is seen as a hypoechoic scalp swelling. The straight sinus may be vertically oriented. It is often associated with other intracranial abnormalities. The presence of venous connection between the scalp lesion and the superior sagittal sinus is a characteristic of sinus pericranii and differentiates it from atretic cephalocele (Fig. 6.13).

6.4 Sonoanatomy of the Normal Spine

The spine has to be examined in all three planes. The sagittal and axial planes are best examined with a layer of amniotic fluid over the dorsum of the fetus. This enables visualisation and study of the overlying skin and subcutaneous layers. This is an integral part of the examination of the spine. The skin and subcutaneous layers cannot be well visualised if the dorsum is apposed to the uterine wall (Fig. 6.14). Whenever possible, high-frequency linear transducer must be used to obtain high-resolution images. If the spine (especially the lumbosacral region) is deep and located just above the

internal os, one may use transvaginal ultrasound to advantage (Fig. 6.15). Each vertebra is represented by one anterior ossific centre for the body and two posterior ossific centres for the arch.

The following are the ultrasound findings in a normal spine:

6.4.1 Sagittal Section

1. In slightly off midsagittal plane, the spine is seen as two parallel rows of echogenic foci with shadowing. The posterior ossific centres constitute the dorsal row, the median anterior ossific centres form the ventral row (Fig. 6.14).

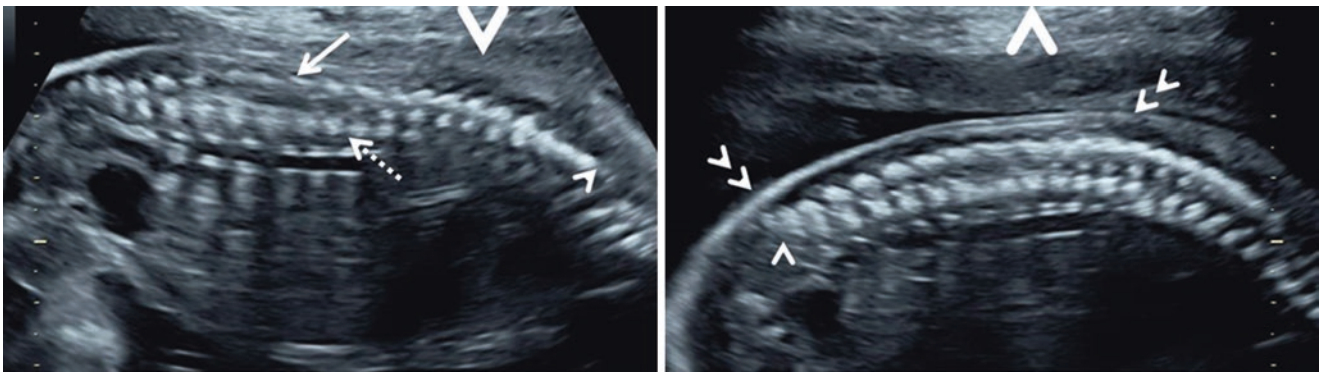

Fig. 6.14 21 weeks (TAS) *paramedian sagittal sections of the normal spine* – posterior ossific centres constitute the dorsal row (solid arrow), the anterior ossific centres constitute the parallel ventral row (dotted arrow), the two rows converge to form the sacral taper with its dorsal uptilt (arrowhead) – in section obtained with probe pressure (large arrow pointing down), the skin outline (double arrowhead) on the fetal dorsum is not seen due to its apposition against the uterine wall; with release of the probe pressure (large arrowhead pointing up), a layer of amniotic fluid seeps in between the fetal dorsum and the uterine wall enabling the visualisation of the skin continuity (double arrowhead)

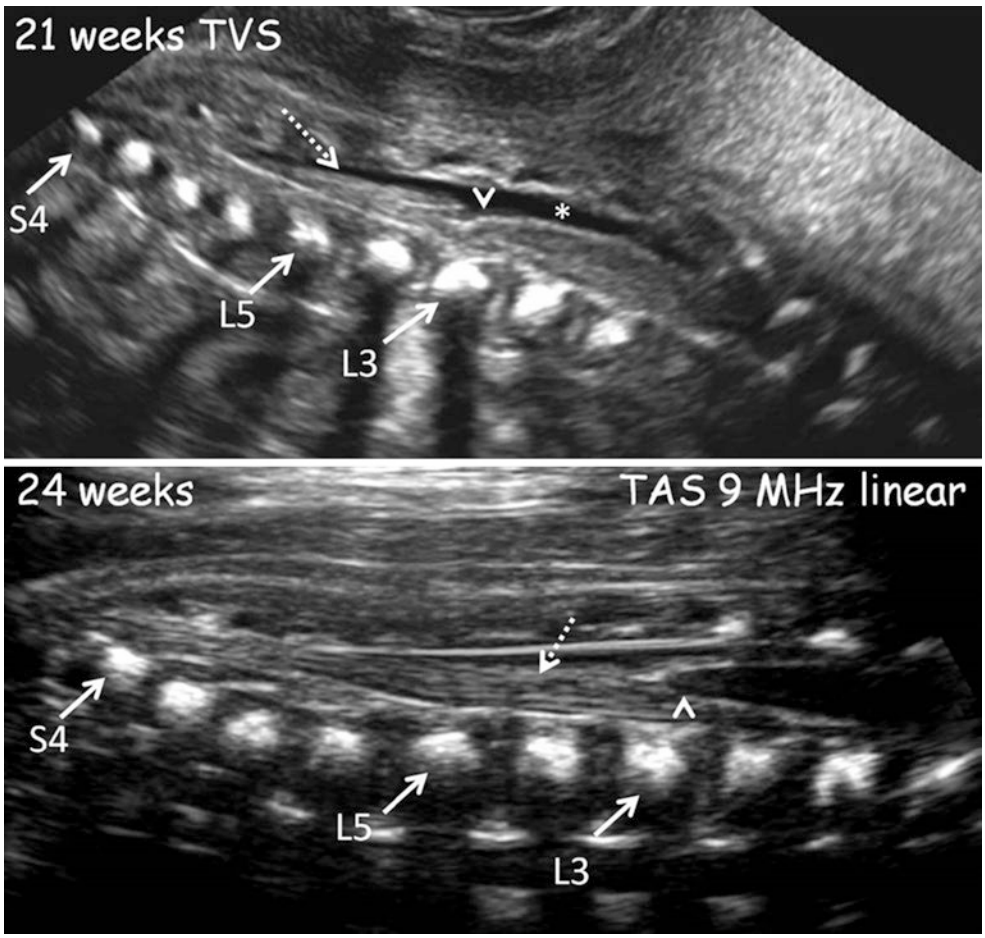

Fig. 6.15 21 weeks (TVS) and 24 weeks (TAS 9 MHz linear) – *midsagittal section of the normal lumbosacral spine* – only the anterior ossific centre row is seen (solid arrows), the posterior ossific centres are not seen as they are paramedian, conus medullaris (arrowhead), cauda equina (dotted arrow), CSF in the vertebral canal (*). The conus medullaris is at the lower border of L3 body. Counting is done from the last sacral segment (S4) cephalad or from T12 caudad

2. The two rows converge in the sacrum to its tip and this is termed the sacral taper.
3. The sacral tip is subtly angled dorsally. This is termed the sacral uptilt.
4. Acoustic shadowing from the ossific centres indicates normal mineralisation.
5. The height of the vertebral body is more than the intervertebral disc space.
6. The skin and subcutaneous layers are intact and continuous over the entire length of the spine.
7. The entire length of the spine in late second and third trimesters cannot be visualised in a single image. Two or more sections are necessary for a complete study.
8. In a true midsagittal section, the beam passes in between the posterior ossific centres, and hence only one row of anterior ossific centres is seen. The spinal cord is best visualised in this section. The spinal cord is seen as a hypoechoic structure with a central echogenic line representing the central canal. The spinal cord runs ventrally in the vertebral canal (Fig. 6.15).
9. The spinal cord tapers and ends as the conus medullaris. In the second trimester, the tip of the conus is at the L2 or L3 levels. The vertebral levels are counted from the lowest ossified sacral centre (S4 in the mid trimester) moving cephalad or from T12 segment (identified by the last rib) moving caudad.
10. The echogenic cauda equina is seen caudal to the conus medullaris.
11. The distance between the tip of the conus and the last sacral ossified body is the conus distance. This distance increases with gestational age and bears a linear relation to the femur length. In cases of tethered cord, the conus distance is less than 5th percentile.

6.4.2 Axial Section

1. Each vertebral segment is represented by three echogenic ossific centres, one median anterior ossific centre and two paramedian posterior ossific centres (Fig. 6.16).
2. These centres are equidistant from each other, and hence straight lines connecting them form an equilateral triangle.
3. The vertebral canal is enclosed by the three dots and contains the spinal cord. It is seen as a hypoechoic circular structure with a central echogenic dot representing the central canal.
4. Skin and subcutaneous layer is intact and continuous over the dorsum.
5. The transducer is swept craniocaudally to serially study the axial sections of all segments from C1 to S4.

6.4.3 Coronal Section

1. In a coronal section, obtained at a slightly ventral plane through the anterior ossific centres, one row of echogenic foci with shadowing is seen.
2. In a section, obtained slightly dorsally through the posterior ossific centres, two parallel rows of echogenic foci with shadowing are seen. This is termed the 'railroad' appearance (Fig. 6.17).
3. In the thoracic spine, parts of the ribs may be seen on either side of the vertebrae.
4. Skin and subcutaneous layer continuity over the spine cannot be studied in this plane.
5. Due to the normal thoracic kyphosis and lumbar lordosis, more than one coronal sections are necessary to study the full length of the spine.
6. The posterior ossific centres converge to the sacral tip.

6.5 Spina Bifida

Segmental failure of closure of the neural tube results in defective fusion of the bony posterior vertebral arch elements. This is commonest in the lumbosacral region followed by sacral, thoracolumbar and cervical regions. The defect is classified as 'open' if there is discontinuity in the skin and subcutaneous layer over the defect (85–90%). The dural tube is exposed to amniotic fluid. It is classified as 'closed' if the defect is covered with skin (10–15%). In open spina bifida (OSB), CSF leaks through the defect into the amniotic cavity. This leads to herniation of the vermis, cerebellar tonsil and medulla oblongata through the foramen magnum and is termed the Chiari II malformation (Fig. 6.18). In closed spina bifida (CSB), there is no CSF leak into the amniotic cavity and the intracranium is normal. Diabetic and obese mothers are at high risk for spina bifida. Mothers on antiepileptic drugs (valproic acid, carbamazepine), warfarin or vitamin A are also at high risk for OSB. Recurrence risk is 1.5–3.0%. Periconceptional folic acid therapy prevents recurrence in subsequent pregnancies.

Feature	OSB	CSB
Percentage of cases	85–90%	10–15%
Neurulation defect	Primary	Secondary
Skin cover	Absent	Present
CSF leak	Present	Absent
Chiari II malformation	Present	Absent
Lesions	Meningocele Myelomeningocele	Tethered cord Spinal lipomas Myelocystocele
MSAFP/AFAChE[a]	Elevated	Normal

[a]Maternal serum alpha-fetoprotein/amniotic fluid acetyl cholinesterase

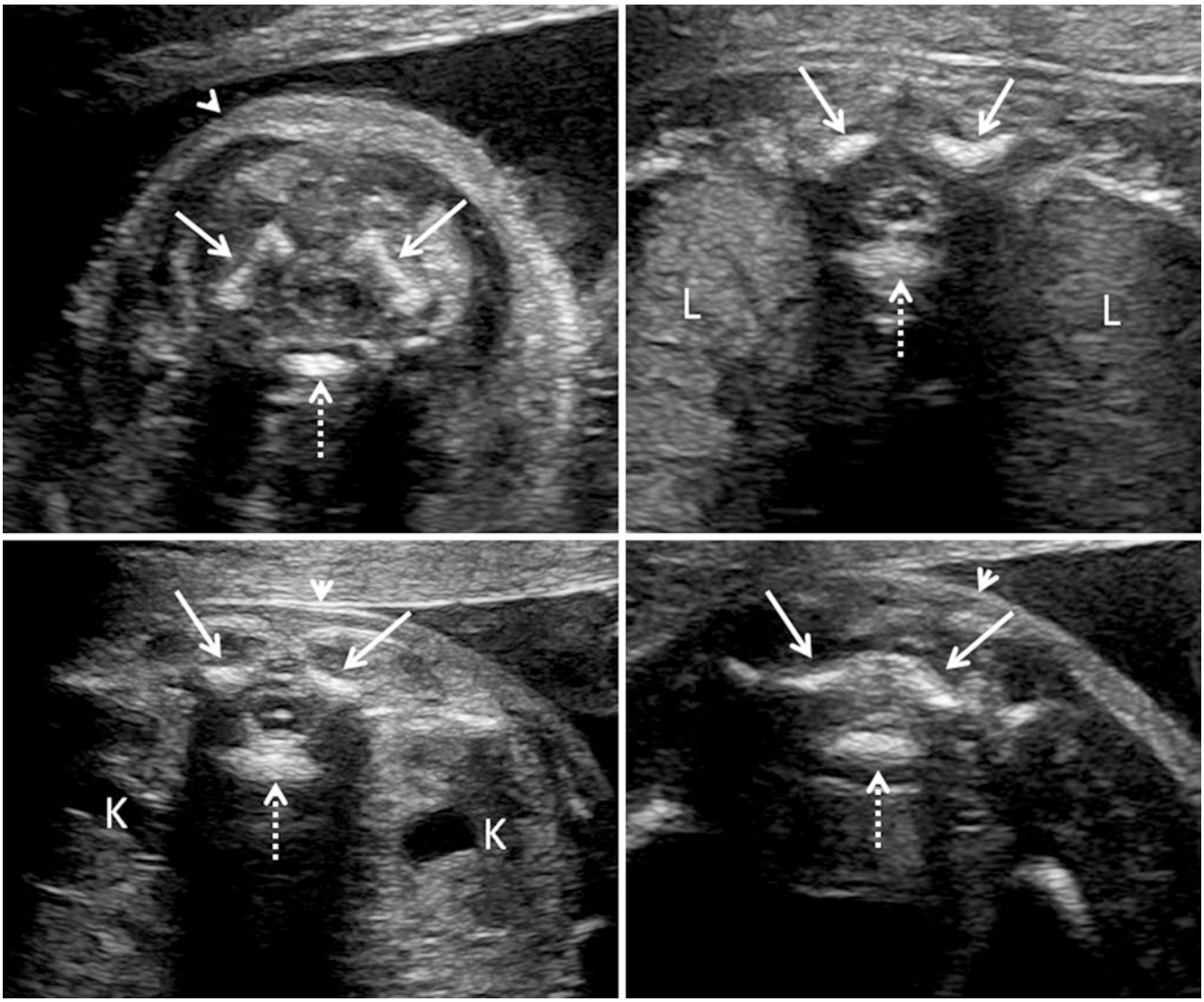

Fig. 6.16 24 weeks (TAS 9 MHz linear) *axial sections of normal cervical, thoracic, lumbar and sacral spine* – two posterior ossific centres (solid arrows), one anterior ossific centre (dotted arrows), the lungs (L), kidneys (K), spinal cord is seen in the vertebral canal as an ovoid hypoechoic structure with a central echogenic dot at all the levels except sacral where the cauda equina is seen as an echogenic region in the vertebral canal, dorsal skin continuity (arrowhead)

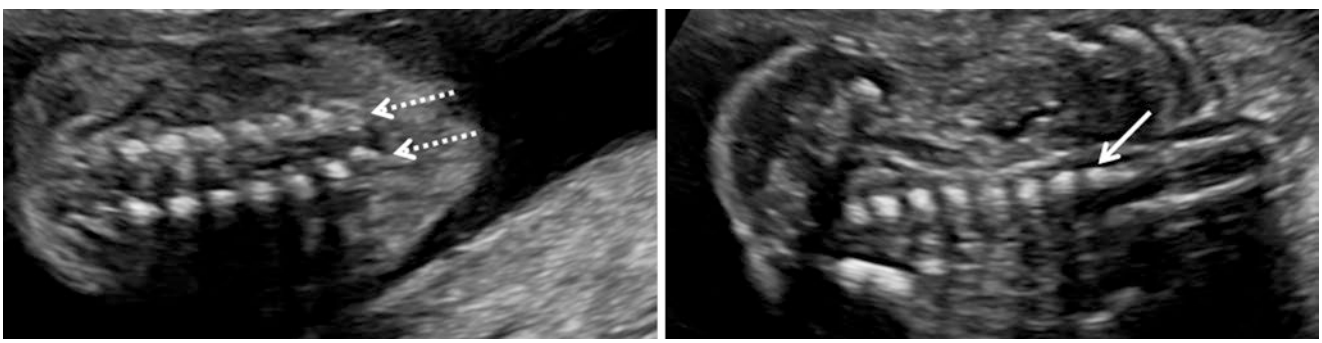

Fig. 6.17 19 weeks (TAS) *anterior and posterior coronal sections of the normal lumbosacral spine* – posterior ossific centres on either side form two parallel rows (rail road appearance) (dotted arrows) – the anterior ossific centres are seen to form a single row in a section obtained slightly anteriorly (solid arrow). Only the lumbosacral region is seen in this section due to the normal spinal curvature

The following are the open lesions:

- Meningocele: The meninges herniate through the dorsal spinal defect to form a cystic mass containing CSF.
- Myelomeningocele: A meningocele with spinal cord or nerve roots or both is termed a myelomeningocele.

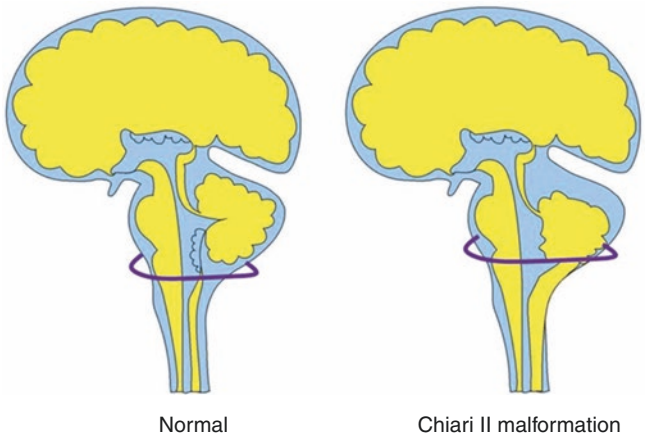

Fig. 6.18 Schematic line diagrams of the posterior cranial fossa changes in Chiari II malformation. The brainstem, fourth ventricle and cerebellar tonsils descend past the foramen magnum

- Myeloschisis: The spinal cord (neural placode) is open and flat, instead of being cylindrical, and is flush with the edges of vertebral arch and the skin defect. No cystic lesion overlies the vertebral defect and no membrane covers the neural placode. In some cases, fluid collection in the vertebral canal beneath the neural placode results in a cystic lesion with elevation of the placode. Taut nerve roots span the cystic lesion in an anteroposterior direction (Fig. 6.19).

The following are the closed neural tube defects:

- Meningocele, lipomyelomeningocele and lipomyeloschisis with skin cover (Fig. 6.19).
- Terminal myelocystocele: The central canal of the spinal cord is dilated and herniated through a spinal defect in the lumbosacral region. Nerve roots are not seen in the cystic lesion. Skin covering is present.
- Lipoma, tethered cord, diastematomyelia, anterior meningocele, neurenteric cyst and spinal dermal sinus: These lesions are not associated with a mass dorsal to the defect.

Fig. 6.19 Schematic line diagrams of open and closed neural tube defects. Meningeal sac (black line), spinal cord and nerves (mauve), vertebral ossification centres (blue), skin (orange), paraspinal muscle (green), lipoma (black ovoid)

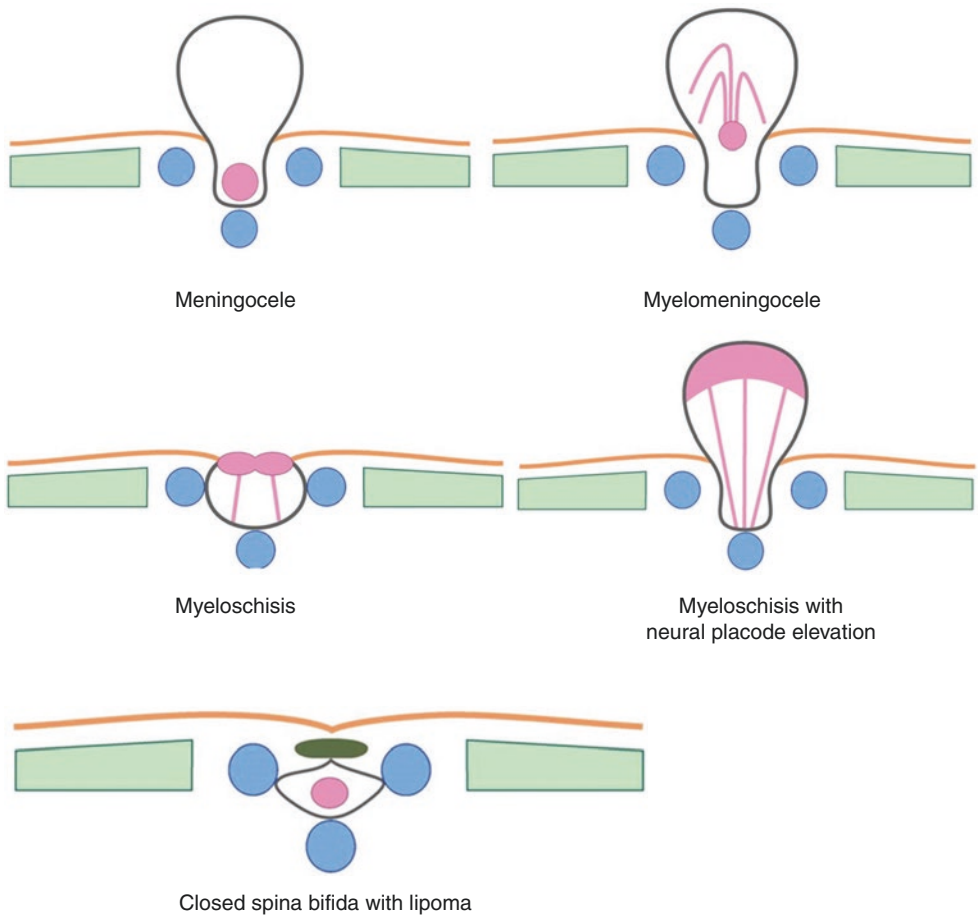

6.5.1 Open Spina Bifida

The ultrasound findings of OSB may be dealt under spinal, intracranial and other findings.

Spinal Findings

1. In axial and sagittal sections, the continuity of skin and subcutaneous layer over the dorsal vertebral defect is interrupted. Presence of amniotic fluid over the lesion is essential to recognise the skin discontinuity.
2. Splaying of the posterior ossific centres of the affected vertebral segments is seen on axial and coronal sections. In axial sections, the affected vertebral segments have a 'U' or 'V' configuration. The posterior ossific centres appear everted (Fig. 6.20).
3. The row of posterior ossific centres seen in the sagittal section is interrupted in the region of the defect (Figs. 6.23 and 6.25).
4. The level of the most rostral segment of the defect is termed the level of the lesion.

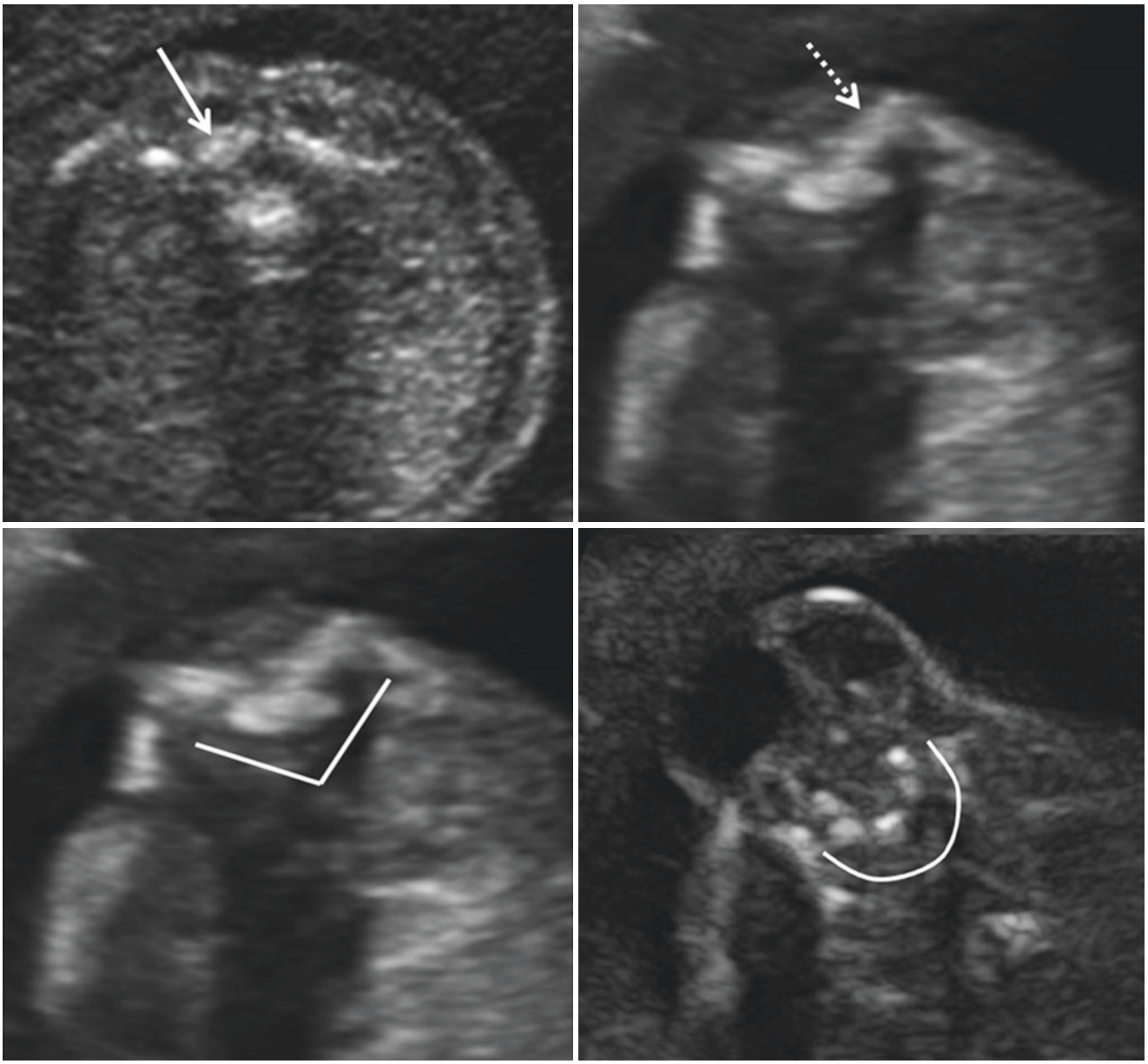

Fig. 6.20 22 weeks (TAS) *normal spine and lumbar open spina bifida* – axial sections of the lumbar spine – normal inward orientation of the posterior ossific centres (solid arrow), outward or everted orientation seen in open spina bifida (dotted arrow), 'V' or 'U' configuration in the vertebral ossific centres in open spina bifida. Note the lack of skin continuity over the lesion

5. Meningocele, myelomeningocele and myeloschisis with elevation of the neural placode result in thin-walled cystic lesions that overlay the vertebral defect. There are no nerve roots in a meningocele. Nerve roots are seen as fine echogenic linear structures in the cystic lesion and are present in myelomeningocele (Figs. 6.21 and 6.22) and myeloschisis with neural placode elevation (Figs. 6.21, 6.23, and 6.24). The cystic lesion is measured in all three planes. Differential diagnosis of sacrococcygeal teratoma should be considered. This lesion is not associated with Chiari II malformation.
6. There is no cystic lesion overlying myeloschisis with flat neural placode (Fig. 6.25). The lesion can be easily missed if the fetus is in spine posterior position or if the dorsum of the fetus is opposed to the uterine wall.
7. Tethered cord is diagnosed when the conus medullaris extends beyond the inferior border of L3 segment in the second trimester (Figs. 6.23 and 6.25).
8. Kyphosis (Fig. 6.26), diastematomyelia (Fig. 6.25) or hemivertebra may be present.
9. 3D rendered or volume contrast imaging with thick slice setting in the coronal plane will facilitate the recognition of the defect and the lesion level. A cystic lesion when present can be displayed by surface rendering. Presence of amniotic fluid around the lesion is essential for surface rendering.

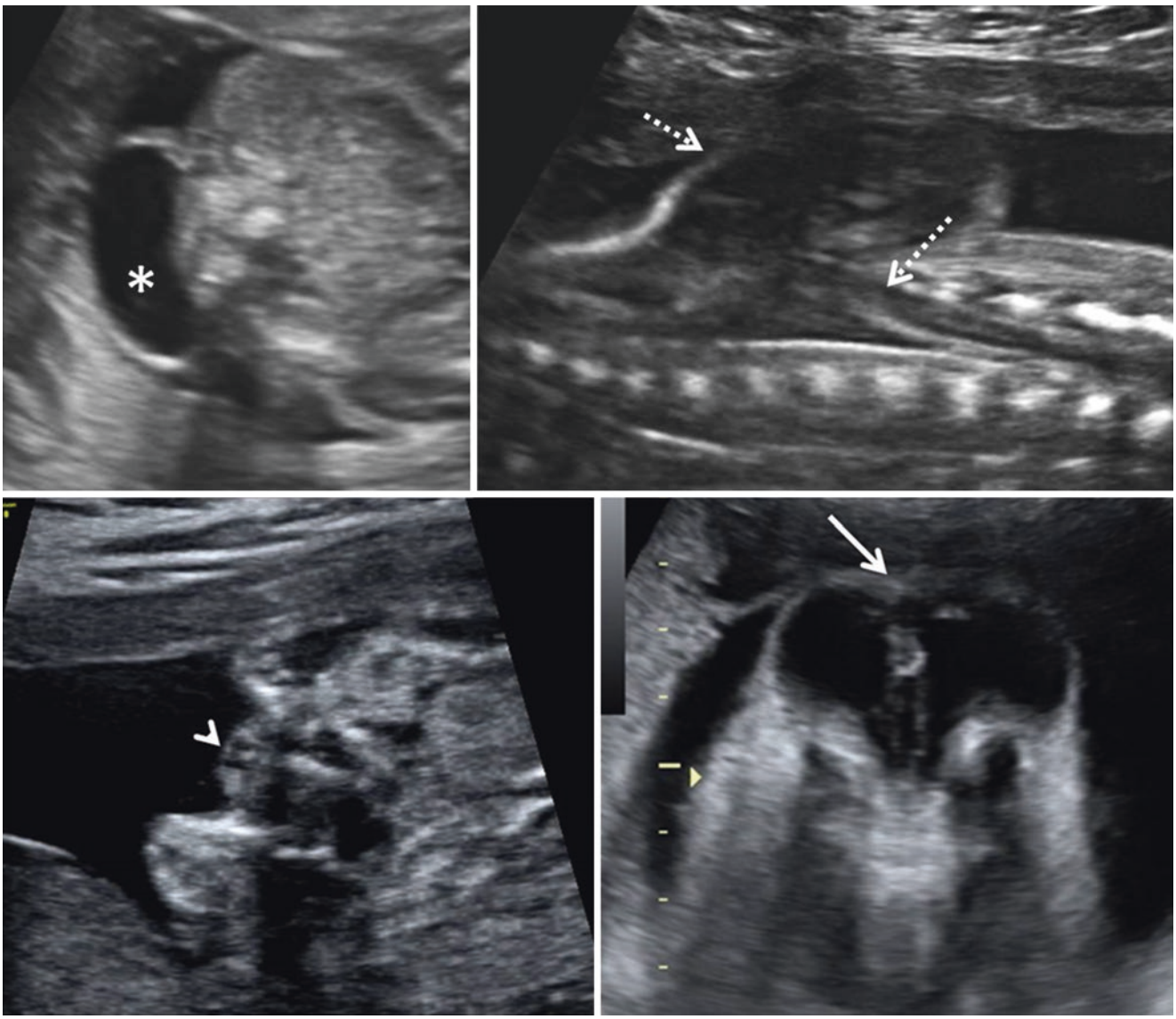

Fig. 6.21 20–24 weeks (TAS) *Various types of OSB* – axial and sagittal sections of the spine – meningocele (*), myelomeningocele with spinal cord and nerve roots in the lesion (dotted arrows), myeloschisis with flat neural placode (arrowhead) and no cystic lesion and myeloschisis with elevated neural placode and presence of a cystic lesion with taut nerve roots (solid arrow)

Intracranial Findings

The intracranial findings serve as important clues to look for OSB.

1. Bilateral frontoparietal flattening or inward scalloping of the calvarium results in the 'lemon sign'. This sign is seen in almost all cases of OSB before 24 weeks (Figs. 6.22, 6.23, 6.25 and 6.27a). In the third trimester, the sign disappears possibly due to modelling and maturation of the calvarial bones. The lemon sign is also seen in about 1% of normal fetuses.
2. Abnormal, sausage-shaped, deformed cerebellum is termed the 'banana sign'. The cisterna magna is obliterated. This sign is seen in about 96% of cases of OSB and is due to Chiari II malformation. The posterior fossa tends to be small (Figs. 6.22, 6.23, 6.24, 6.25, 6.26 and 6.27a).
3. The BPD and HC are less than 5th percentile in 62% and 35% of cases of open spina bifida, respectively.
4. Lateral ventriculomegaly is seen in about 54% of cases, mostly in the third trimester (Figs. 6.22, 6.23 and 6.26).
5. Other supratentorial findings in OSB in the second and third trimesters:

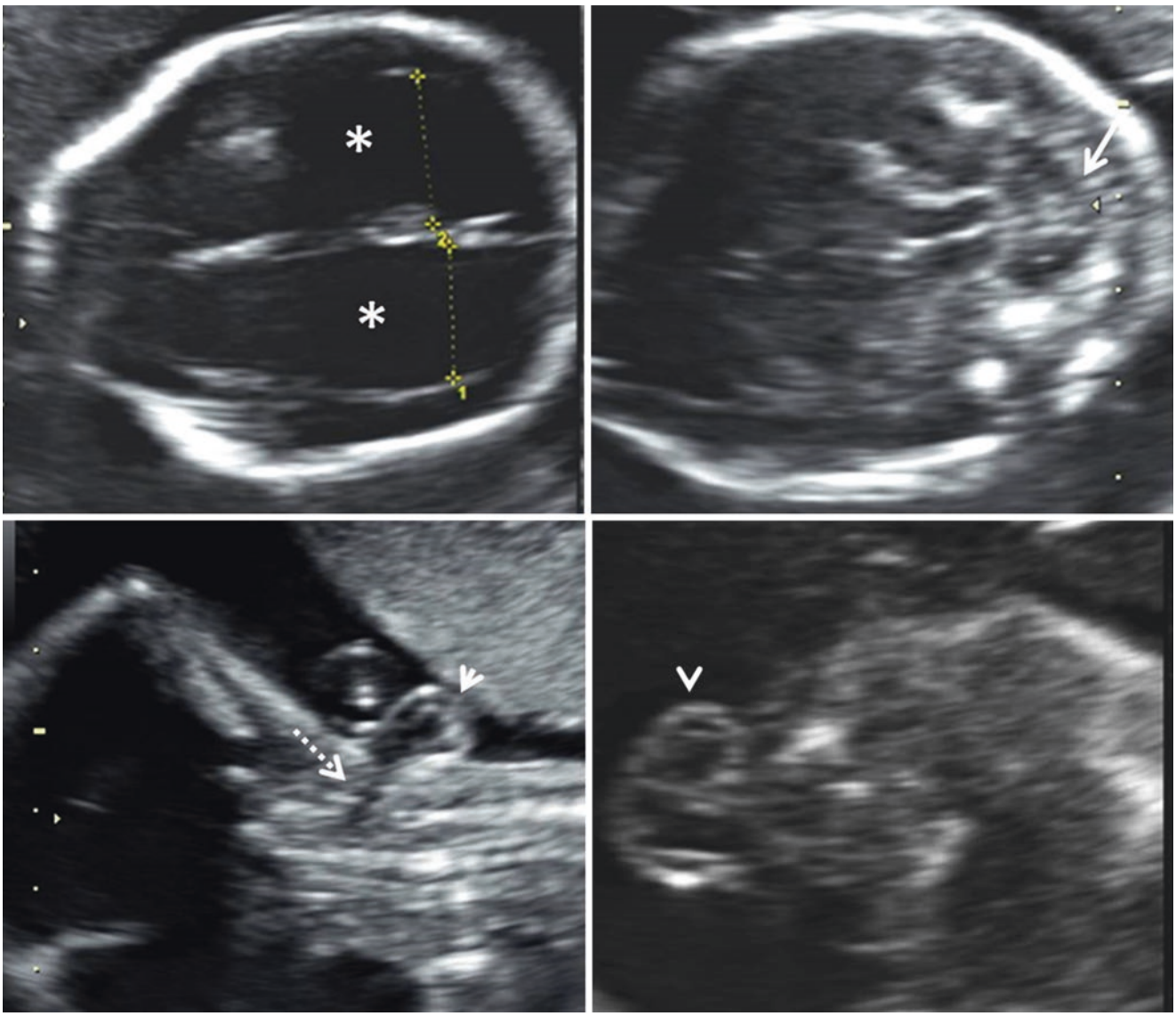

Fig. 6.22 21 weeks (TAS) *single segment cervical open spina bifida with myelomeningocele, Chiari II malformation and lateral ventriculomegaly* – axial transventricular and transcerebellar sections of cranium, sagittal and axial sections of cervical spine – bilateral lateral ventriculomegaly (*), deformed cerebellum with obliteration of cisterna magna (banana sign) (solid arrow), myelomeningocele without skin cover (arrowheads), the track connecting the myelomeningocele to the vertebral canal is arising at C3–C4 level (dotted arrow)

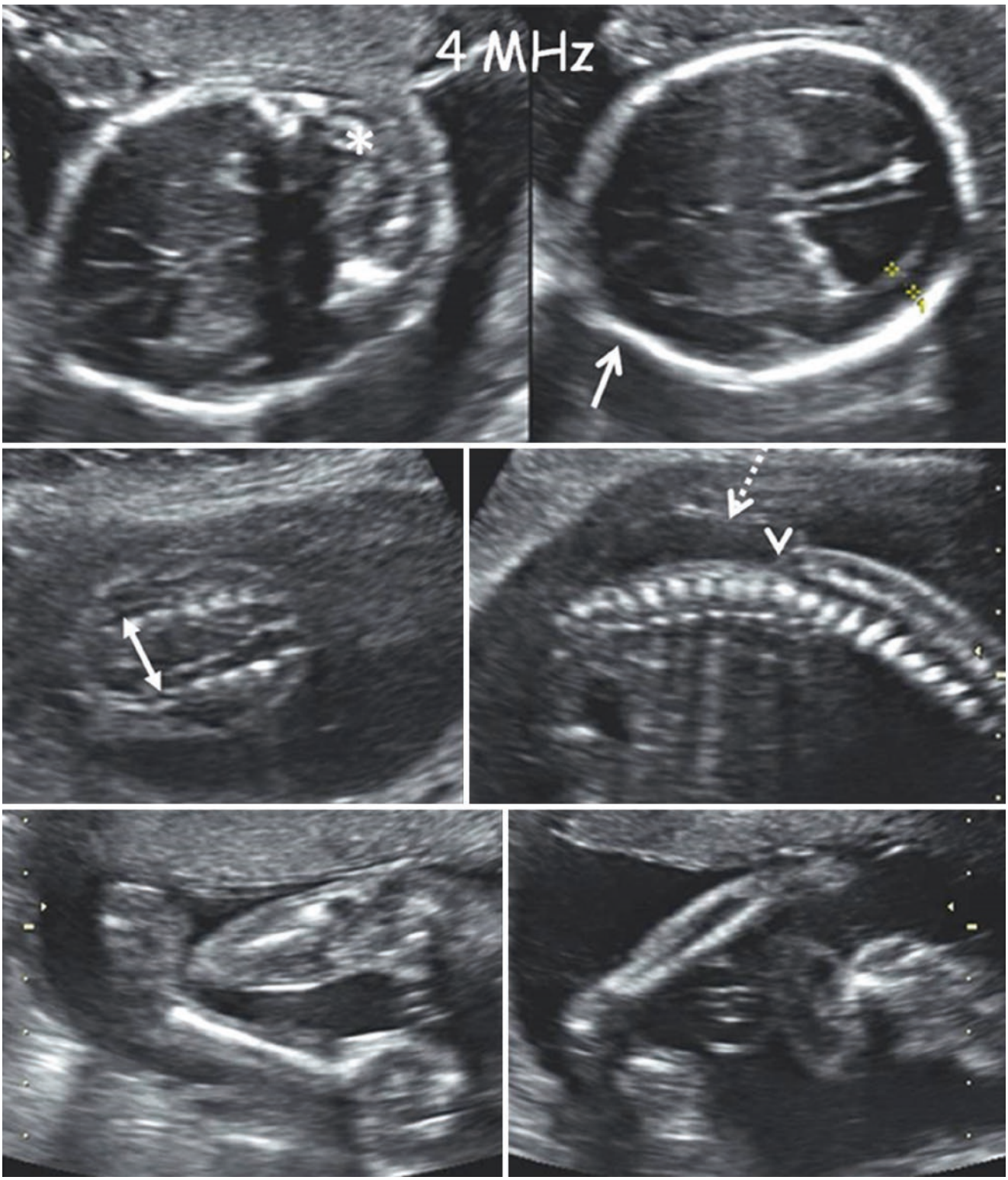

Fig. 6.23 23 weeks (TAS 4 & 9 MHz) *lumbosacral open spina bifida, myeloschi-sis with elevated neural placode, tethered cord and Chiari II malforma-tion* – axial transcerebellar and transventricular cranial sections, coronal and sagittal sections of lumbosacral spine and coronal sections of both legs, sagittal and axial sections of lumbosacral spine – 'lemon' sign (solid arrow), 'banana' sign, Chiari II malformation (*) bilateral lateral ventriculomegaly, splaying of the posterior ossific centres in the lumbosacral region with widening of the lumbar canal (double sided solid arrow), neural placode is elevated (dotted arrow) with bridging nerve roots, skin cover is absent, the line of posterior ossific centres is interrupted at T12 level (arrowhead) as counted from S4 cephalad, the lumbar and sacral segments are involved, conus medullaris is coursing dorsally to extend to the elevated neural placode (double arrowheads), bilateral talipes equinovarus

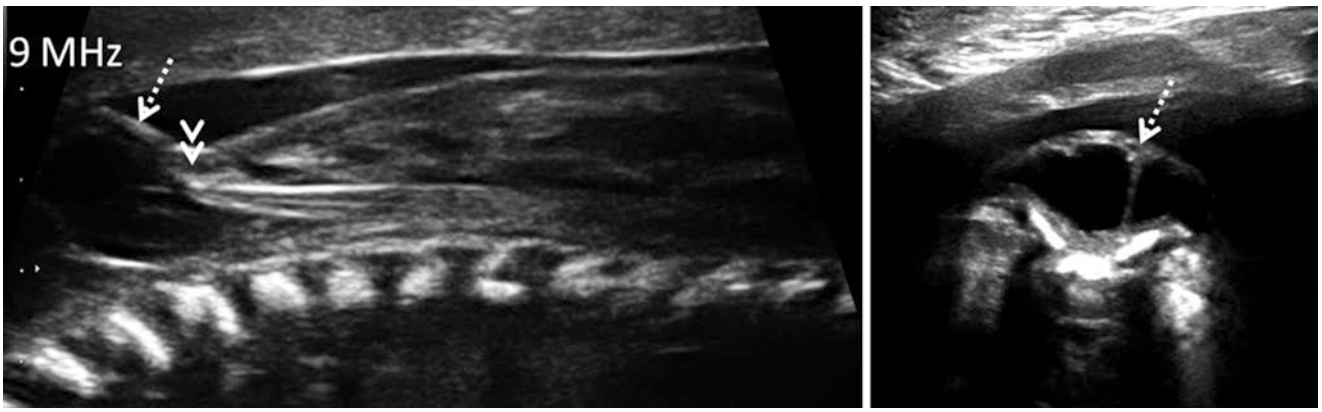

Fig. 6.23 (continued)

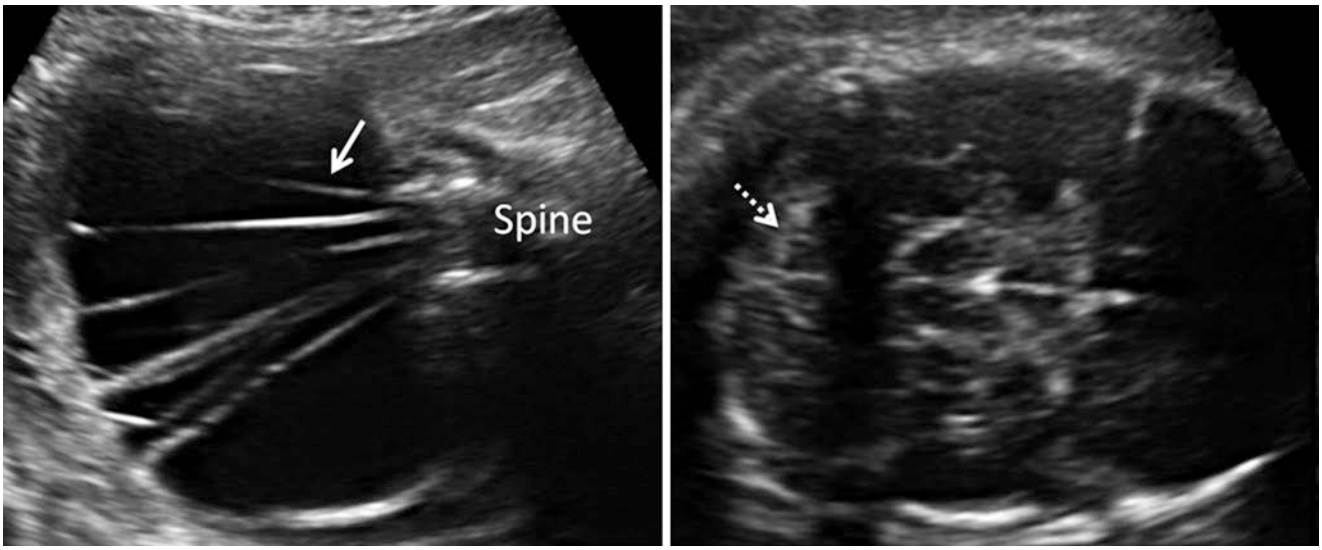

Fig. 6.24 32 weeks (TAS) *lumbar myeloschisis with elevated neural placode and Chiari II malformation* – axial section of lumbar spine and axial transcerebellar section of the cranium – elevated neural placode with multiple taut spinal nerve roots (solid arrow), Chiari II malformation 'banana sign' (dotted arrow)

(a) Diamond-shaped interhemispheric cystic space is seen posterior to the CSP on axial transventricular sections in 43% of cases of OSB. This cystic space, in midsagittal section, is immediately inferior to the splenium of the CC and is due to a prominent cavum veli interpositi (Figs. 6.27b, 6.28, 6.29 and 6.30). The 'diamond sign' is not related to the gestational age, level of the vertebral lesion or presence of hydrocephalus. The 'diamond sign' may also be seen in cases of occipital encephalocele.

(b) The tectum is beaked posteriorly on axial transthalamic sections and is seen in about 66% of cases of OSB (Fig. 6.27b).

(c) The tip of the posterior horn is pointed and is termed the 'ventricular point sign'. It is seen on axial transventricular sections in 70% of cases of OSB. The pointed tip of the posterior horn is also closer to the cerebral surface. The horn to occipital bone distance is decreased (Fig. 6.27b).

(d) Enlarged massa intermedia (interthalamic adhesion) is seen in OSB on MR midsagittal sections. CC dysgenesis and neuronal migration abnormalities can be recognised if present.

Other Findings

Lower limb neuromuscular sequelae such as talipes (Fig. 6.23), rocker-bottom feet or frank arthrogryposis may be seen. Associated conditions such as Meckel-Gruber syndrome, OEIS complex or cloacal exstrophy must be recognised. Karyotyping is indicated if there are other abnormalities.

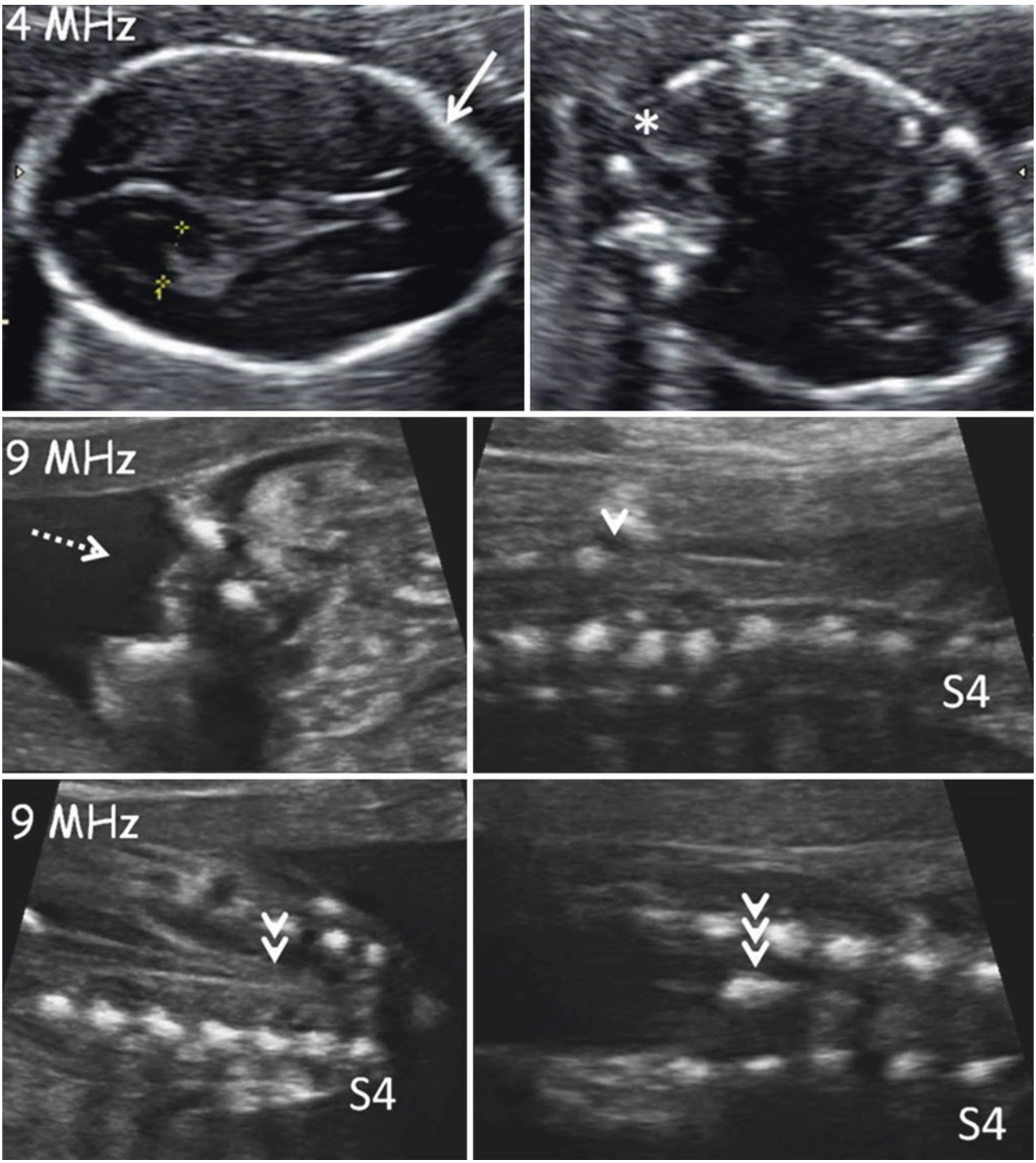

Fig. 6.25 19 weeks (TAS) *lumbosacral open spina bifida (myeloschisis), tethered cord, diastematomyelia and Chiari II malformation* – axial transventricular and transcerebellar sections, axial, sagittal and coronal sections of lumbosacral spine – 'lemon' sign (solid arrow), 'banana' sign, Chiari II malformation (*), splaying of posterior ossific centres in lumbar region with widening of lumbar canal, neural placode is not elevated (dotted arrow), no meningocele seen, skin cover is absent, the line of the posterior ossific centres is interrupted (arrowhead), lesion level is L3 (arrowhead) as counted from S4 cephalad, lumbar and sacral segments are involved, conus medullaris is reaching S2 (double arrowheads) associated midline canal osseous spur seen at S1 level (triple arrowheads)

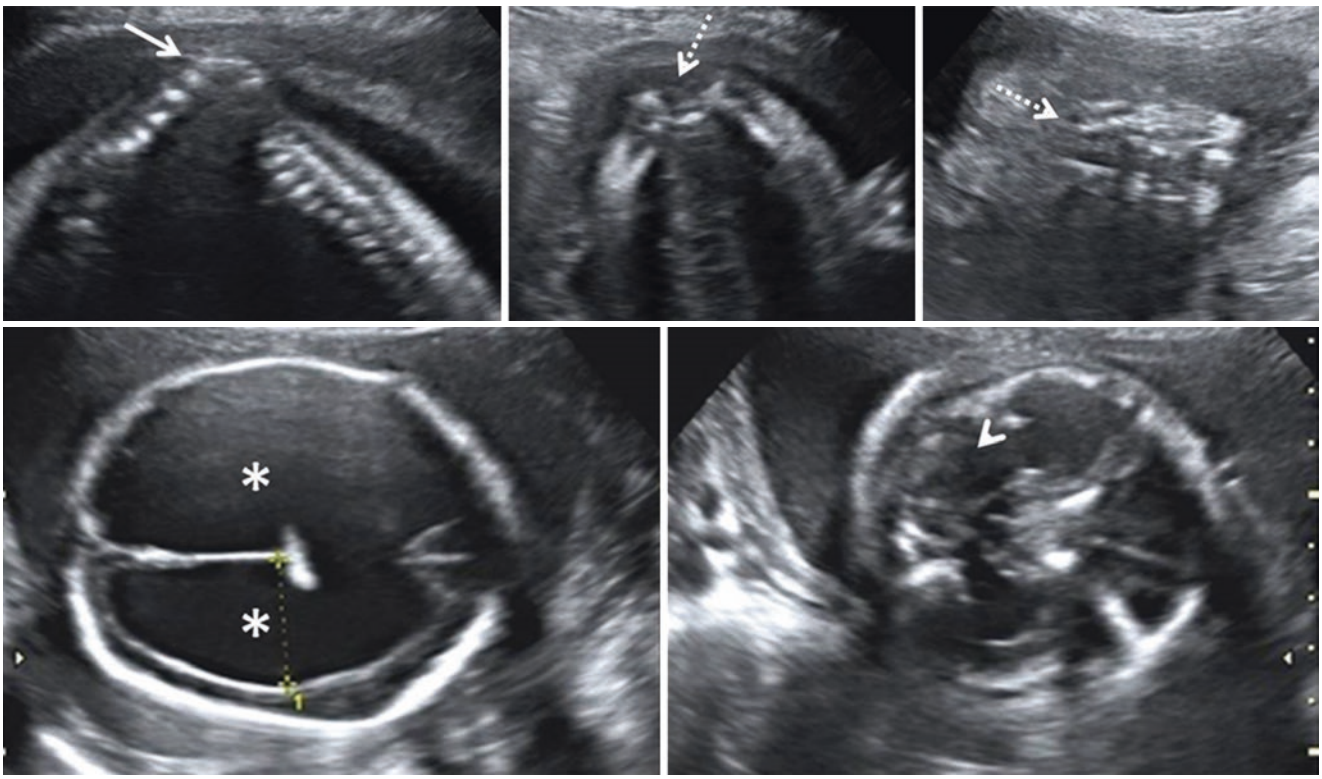

Fig. 6.26 28 weeks (TAS) *lumbosacral open spina bifida with angular kyphosis (gibbus)* – sagittal section of the thoracolumbosacral spine, axial and coronal sections of upper lumbar spine, axial transventricular and transcerebellar sections – gibbus (solid arrow), splaying of posterior ossific centres (dotted arrow), gross bilateral lateral ventriculomegaly (*), Chiari II malformation (arrowhead)

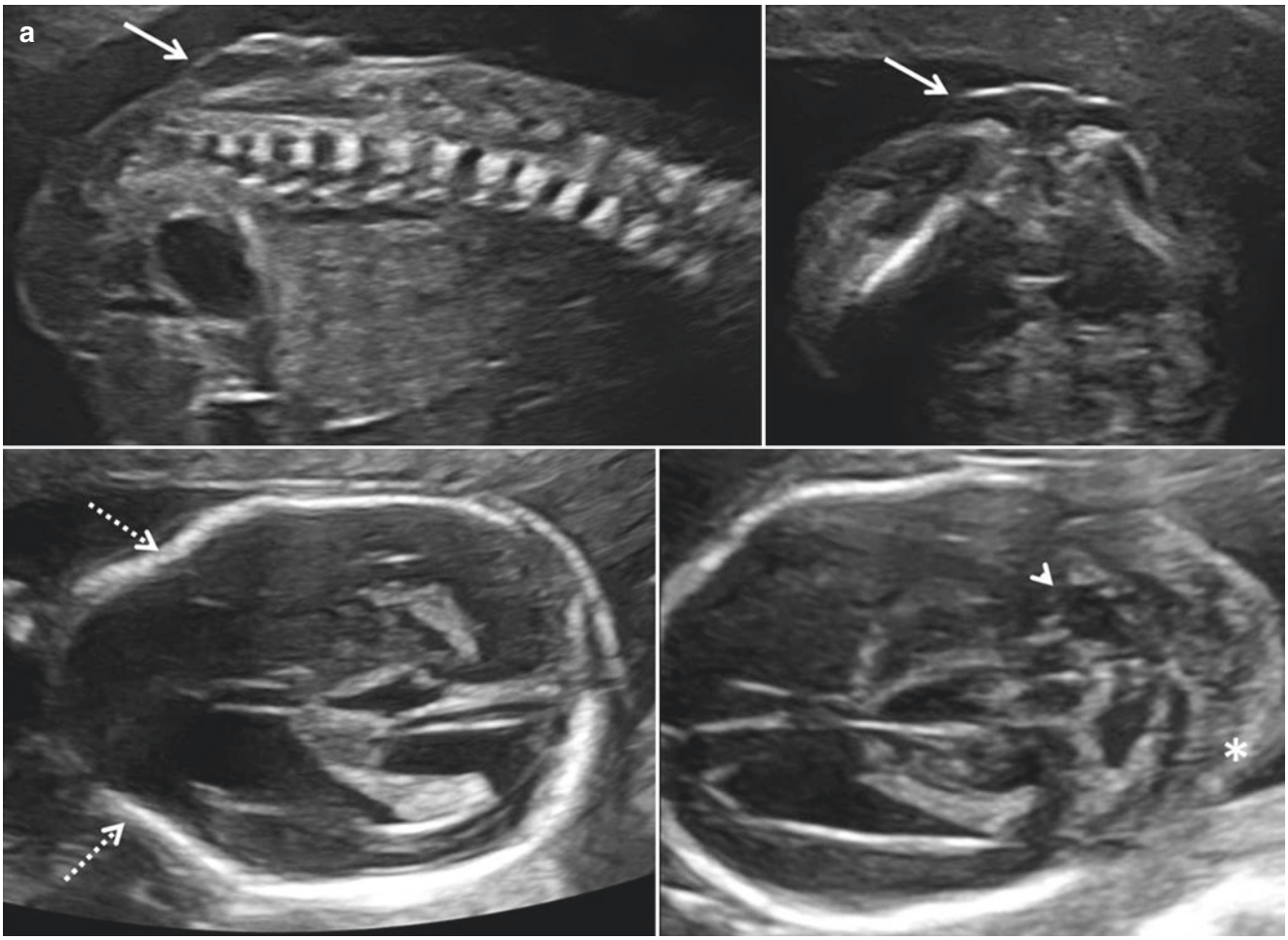

Fig. 6.27 (**a**) 19 weeks (TAS 6 MHz) *lumbosacral open spina bifida with lemon and banana signs* – lumbosacral open spina bifida (solid arrow), 'lemon' sign (dotted arrow), 'banana' sign (arrowhead). (**b**) 19 weeks (TAS 6 MHz) *lumbosacral open spina bifida with supratentorial signs* – 'diamond' sign (solid arrow), beaked tectum (dotted arrow), ventricular point sign (arrowhead), lateral ventricular posterior horn tip is close to the occipital bone (dotted line)

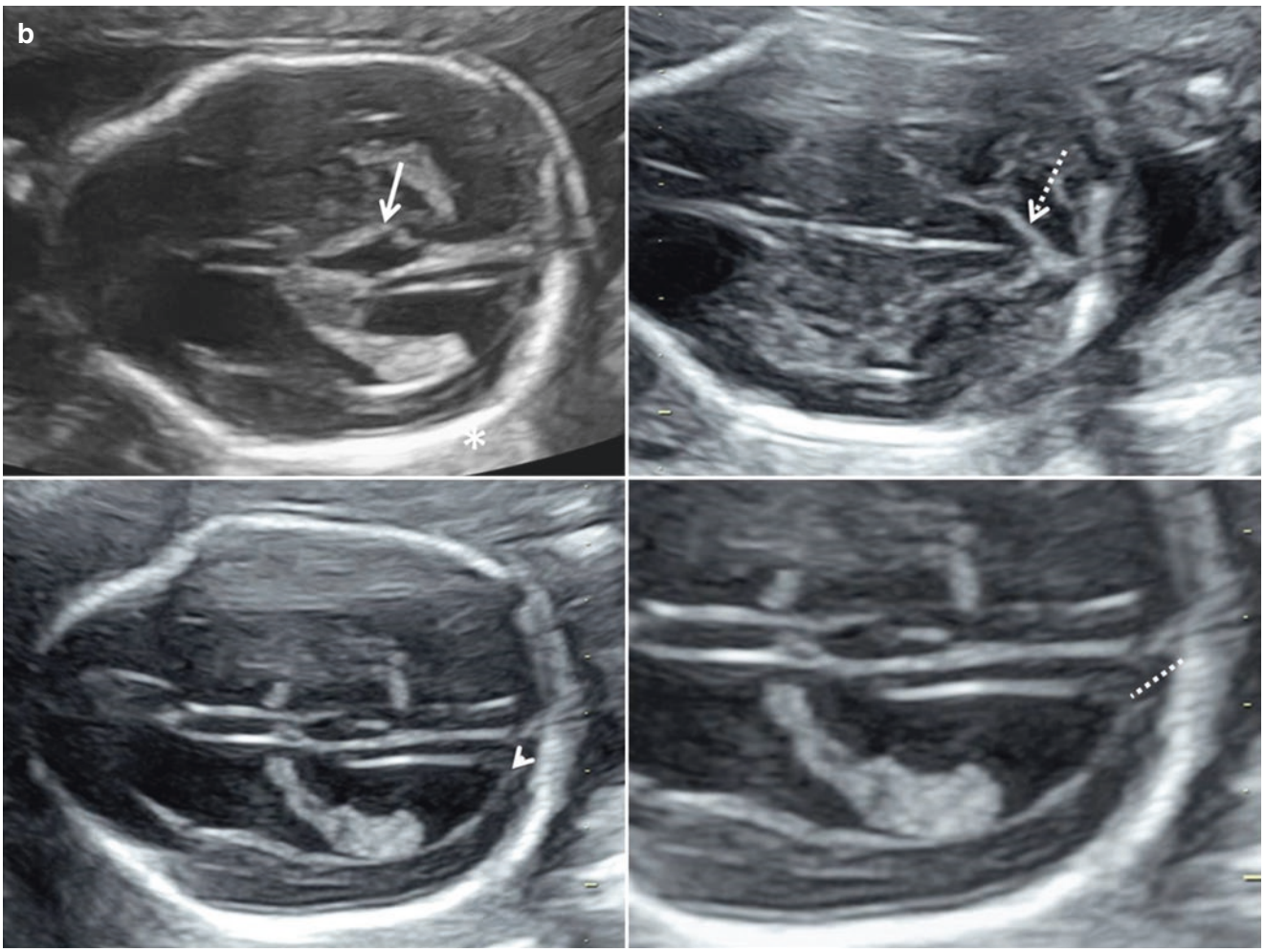

Fig. 6.27 (continued)

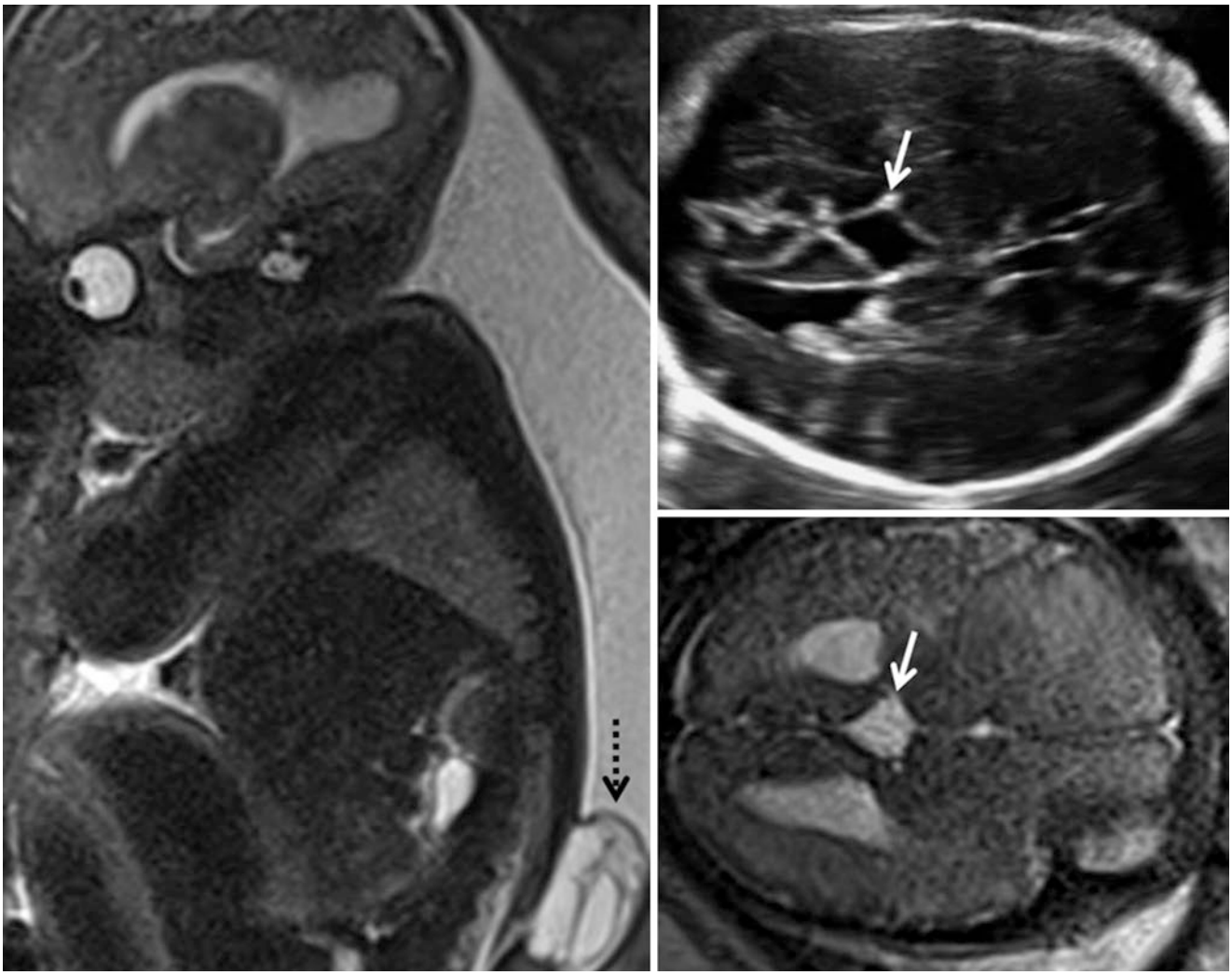

Fig. 6.28 32 weeks (TAS and MRI) *diamond sign in a case of lumbosacral open spina bifida* – 'diamond' sign (solid arrow), lumbosacral myelomeningocele (dotted arrow)

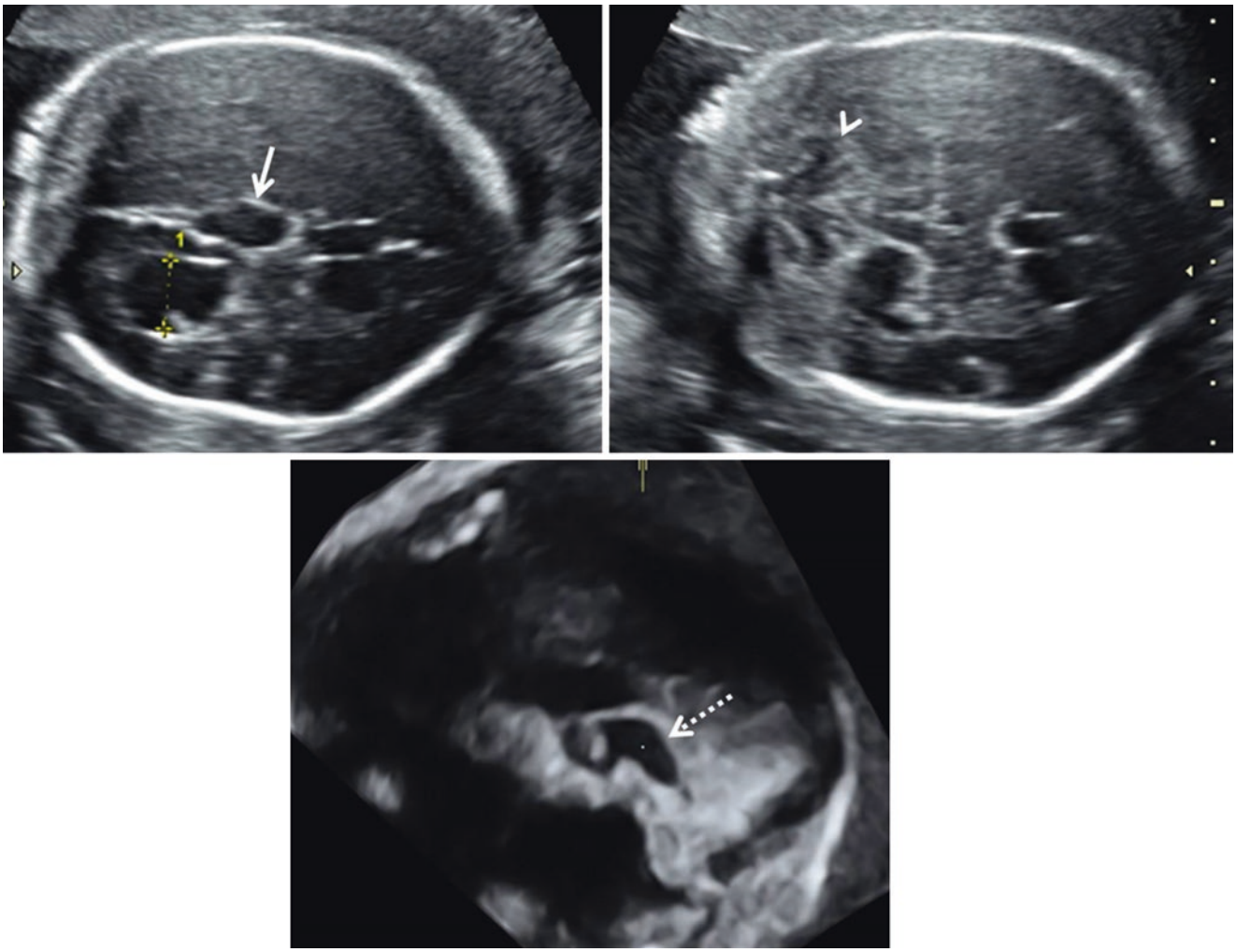

Fig. 6.29 27 weeks (TAS) *diamond sign in a case of thoracolumbosacral open spina bifida* – axial transventricular and transcerebellar sections, 3D midsagittal section – 'diamond' sign (solid arrow), 'banana sign' (arrowhead), typical location of the 'diamond', the prominent cavum veli interpositi inferior to splenium of CC (dotted arrow)

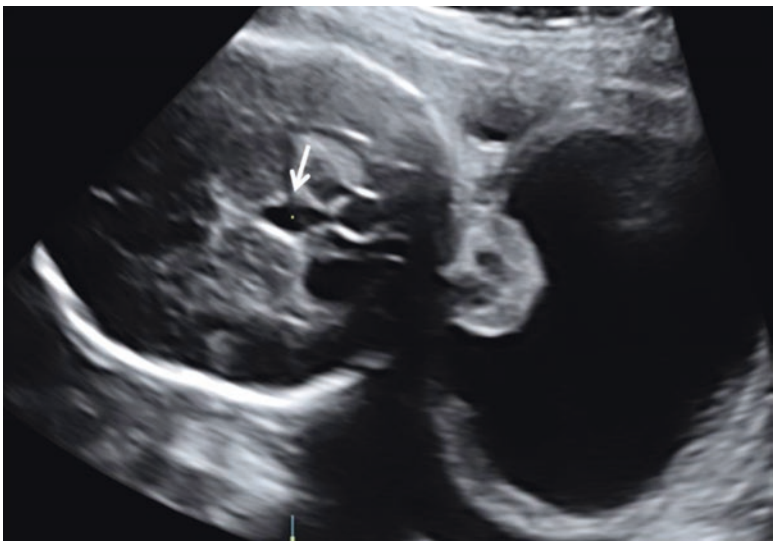

Fig. 6.30 29 weeks (TAS) *occipital encephalocele – with diamond sign* (solid arrow)

6.5.2 Closed Spina Bifida

CSB is difficult to detect as there are no intracranial signs to suspect a spinal defect. Diligent examination of the fetal spine in all three axes is necessary to detect these lesions.

The ultrasound findings are as follows:

1. All cystic lesions (meningocele and myelomeningocele) associated with spinal bifida should be critically examined for presence of skin and subcutaneous tissue cover. This can be done by tracing the continuity of the skin and subcutaneous layers over the defect. The membrane covering the cystic lesion is generally thick when the skin is intact (Figs. 6.31 and 6.32).
2. Presence of lipomatous tissue is recognised as hyperechoic regions seen in the wall of the cystic lesion (Figs. 6.33 and 6.34). When lipomas are associated with flat lesions, they are seen as hyperechoic masses in the intradural and/or the subcutaneous planes. The subcutaneous lipomas are often connected to the vertebral canal by a track through the spinal defect.

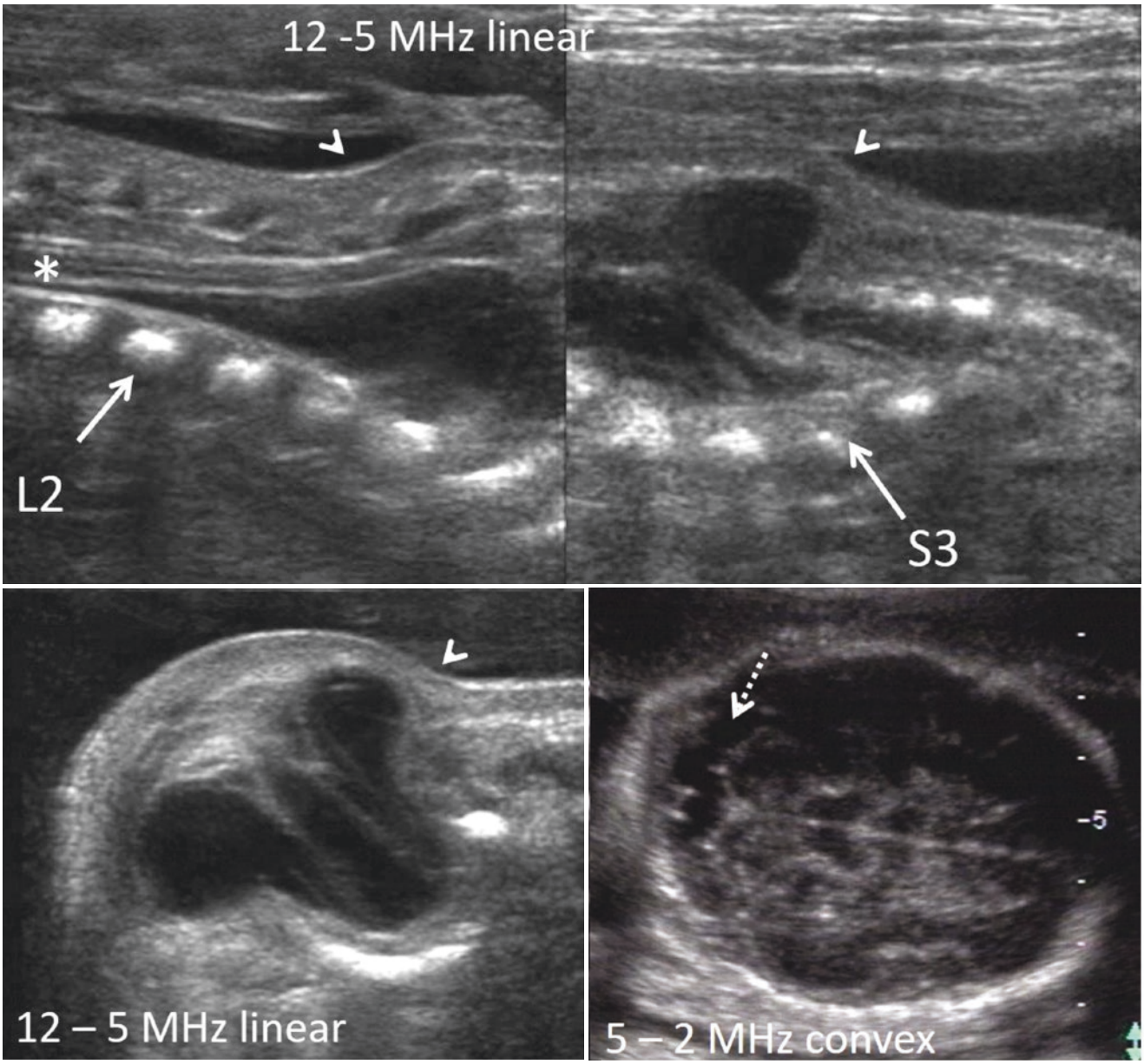

Fig. 6.31 24 weeks (TAS) *lumbosacral closed spina bifida with myelomeningocele* – myelomeningocele (elevated neural placode) with skin covering (arrowheads), lesion level is L2, the spinal cord (*) courses dorsally to extend to the myelomeningocele and is eventually tethered at S3 level, there is no Chiari II malformation (dotted arrow)

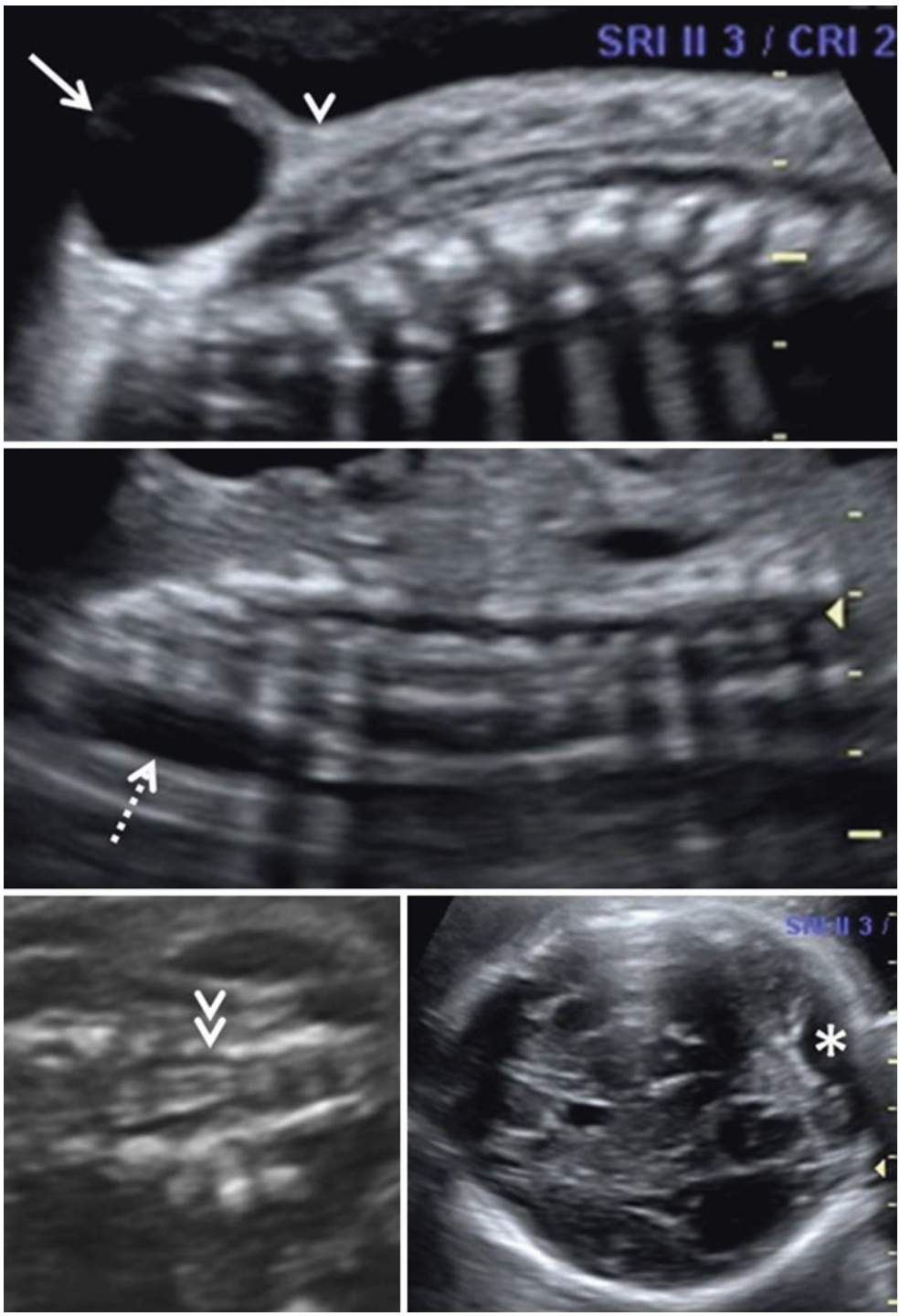

Fig. 6.32 32 weeks (TAS) *sacral closed spina bifida with meningocele and tethered cord* – sagittal sections of lumbosacral spine in spine anterior and posterior positions, coronal section of the lumbosacral spine, axial transcerebellar section of the cranium – meningocele (solid arrow) with intact skin cover (arrowheads), lesion level is S1, conus is at L4 level (double arrowhead) indicating tethering, the meningocele is flattened and almost not recognisable in the spine posterior position of the fetus without surrounding amniotic fluid (dotted arrow), there is no Chiari II malformation (*)

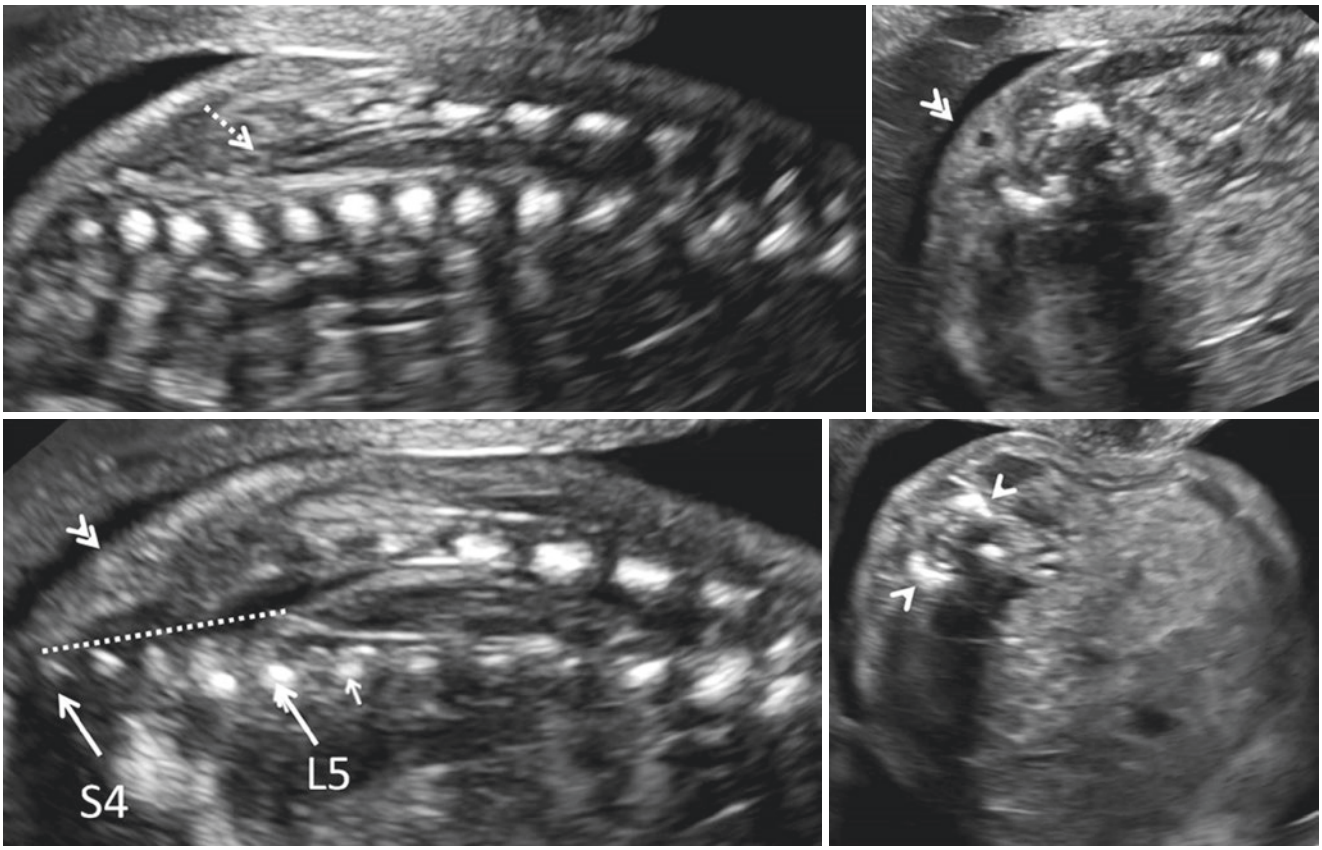

Fig. 6.33 21 weeks (TVS) *sacral closed spina bifida with lipoma* – conus medullaris (dotted arrow) is at L5 level indicating tethered cord, splayed posterior ossific centres (arrowheads), intact skin cover with hyperechoic subcutaneous lipoma (double arrowhead), conus distance (dotted line) is less than 5th percentile. No meningocele seen

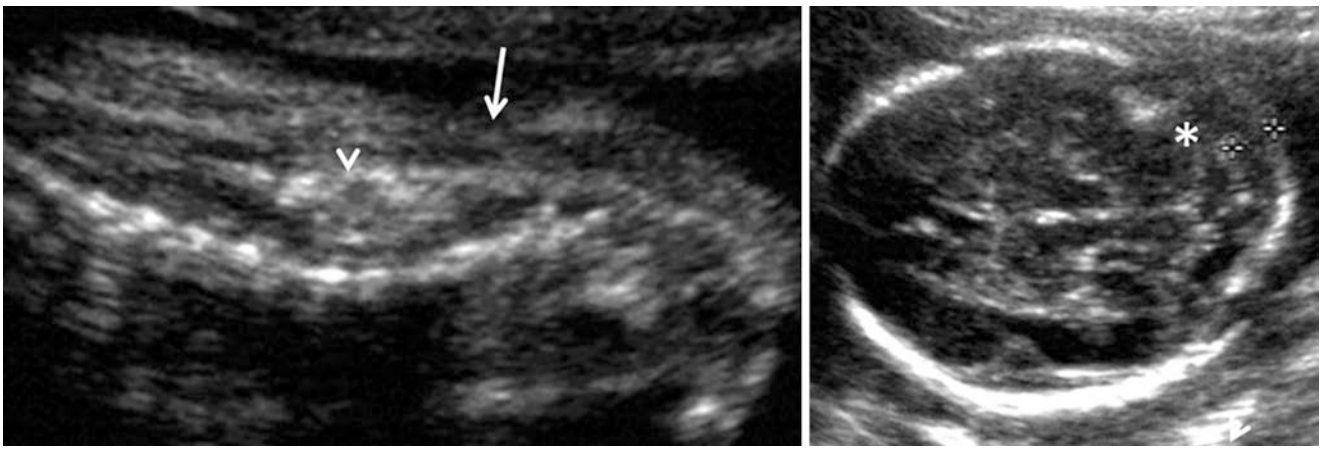

Fig. 6.34 22 weeks (TAS) *lumbosacral closed spina bifida with lipoma* – intact skin and subcutaneous layer (solid arrow), intradural lipoma (arrowhead), no evidence of Chiari II malformation (*). No meningocele seen

3. Presence of tethered cord with splaying of posterior ossific centres and no meningo/myelomeningocele may be identified (Fig. 6.33). The level of conus medullaris is caudal to L3. The conus distance is the distance between the last vertebral body and the conus medullaris. Conus distance less than 5th percentile for the femur length (or FL in mm minus eight) indicates tethered cord.
4. There are no intracranial signs associated with CSB.
5. A terminal myelocystocele is recognised by the presence of the dilated spinal cord central canal ballooning out of the lumbosacral vertebral defect. This can be recognised by tracing the spinal canal with a high-frequency transducer.
6. Associated findings include sacral dysgenesis, hemivertebra, scoliosis and genitourinary abnormalities.

MRI is useful for detecting fat content as well as the presence of skin cover. Recognition of the dilated central canal in myelocystocele is possible with MRI.

6.6 Craniorachischisis

It is the most severe open neural tube defect where there is no closure of the entire neural groove. This results in anencephaly continuous with an open spina bifida involving the entire spine (Fig. 6.35). This occurs in about 10% of the cases of anencephaly.

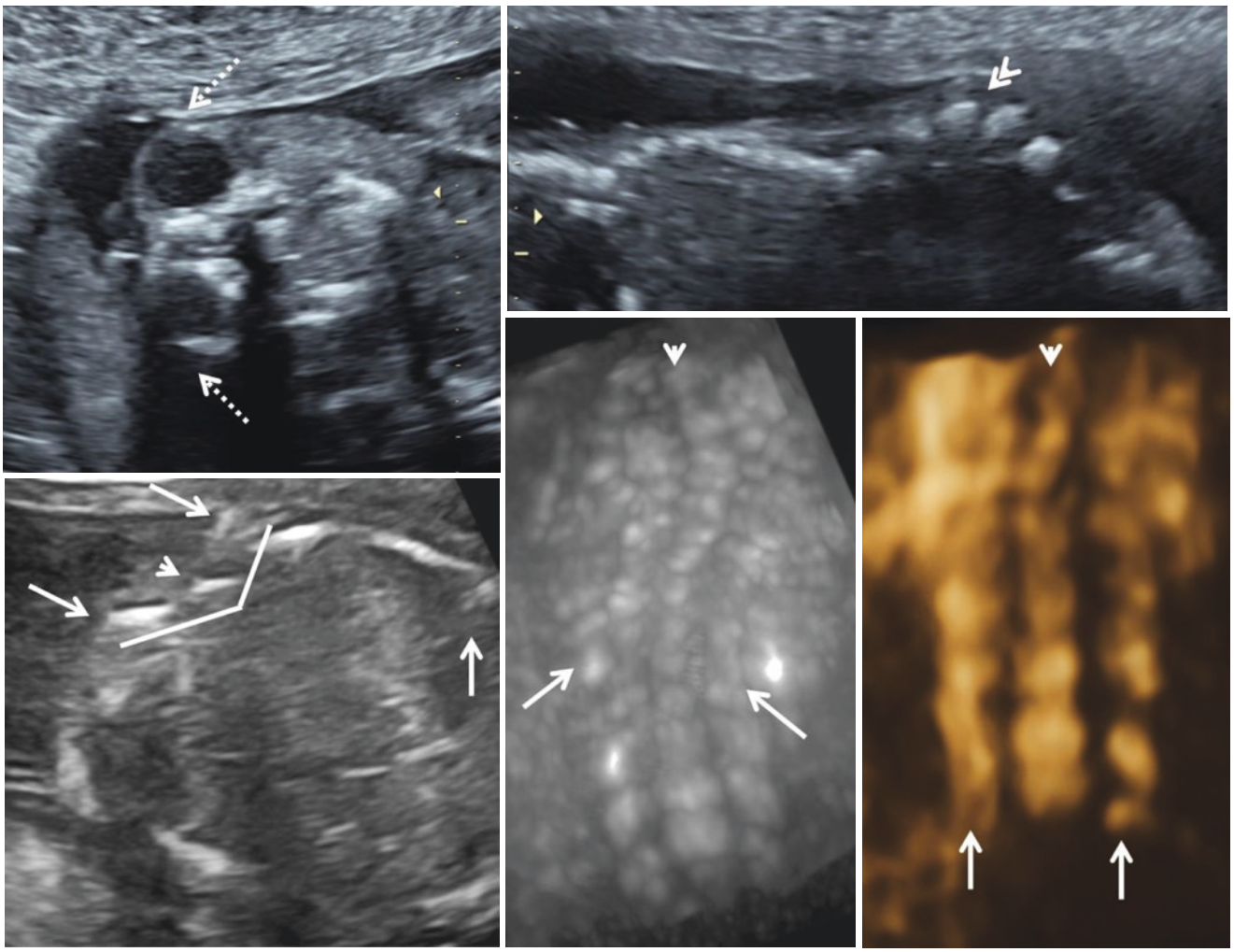

Fig. 6.35 23 weeks (TAS) *craniorachischisis* – axial section through the orbits, sagittal section of the spine, axial section of the lumbar spine and 3D coronal-rendered images of the spine – prominent orbits (dotted arrows), the calvarial bones and intracranium are not seen, kyphoscoliosis (double arrowhead), severe splaying of the posterior ossific centres of the entire spine (solid arrows), the anterior ossific centre (arrowhead) is almost collinear with the posterior centre. The involvement of the entire spine is well appreciated on the rendered images

6.7 Diastematomyelia, Hemivertebra, Neurenteric Cyst and Sacral Agenesis

6.7.1 Diastematomyelia

1. Diastematomyelia is the presence of a bony midline hyperechoic spur in the vertebral canal. The spur may be demonstrated in the axial, coronal and midsagittal sections (Figs. 6.25 and 6.36a, b).
2. Local widening of the vertebral canal results in splaying of the posterior ossific centres.
3. There is no breach in the skin and subcutaneous layers overlying the lesion.
4. One or more segments may be involved. The lesion is most often seen in the thoracolumbar region.
5. Fibrous or cartilaginous spur is not hyperechoic and is not detected on ultrasound.
6. Split spinal cord or conus medullaris can be seen with magnified high-frequency ultrasound images (Fig. 6.36a, b).

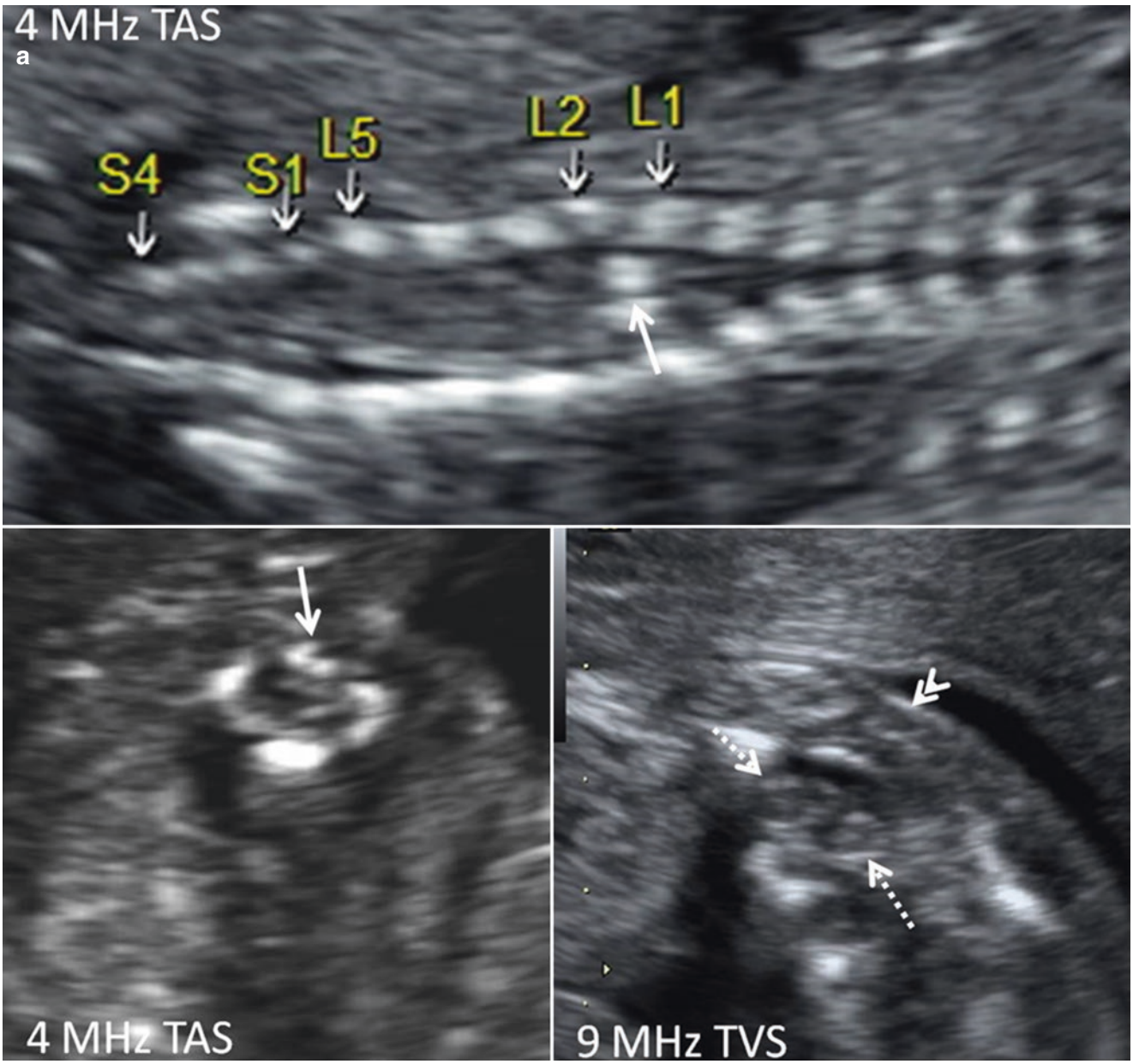

Fig. 6.36 (**a**) 19 weeks (TAS and TVS) *lumbar diastematomyelia with split and tethered cord* – coronal and axial sections of lumbosacral spine – widening of the lumbosacral vertebral canal (splaying of the posterior ossific centres), bony spur seen in the vertebral canal at L1 level (solid arrow), two spinal cords each with a central spinal canal (dotted arrows), skin cover is intact (arrowhead). (**b**) 19 weeks (TVS) *lumbar diastematomyelia with split and tethered cord* – coronal (posterior and anterior), sagittal and 3D coronal VCI views – two spinal cords seen in the vertebral canal from L1 level caudad (dotted arrows), midline vertebral canal bony spur (solid arrow) at L1, conus medullaris is at the level of L5 (arrowhead)

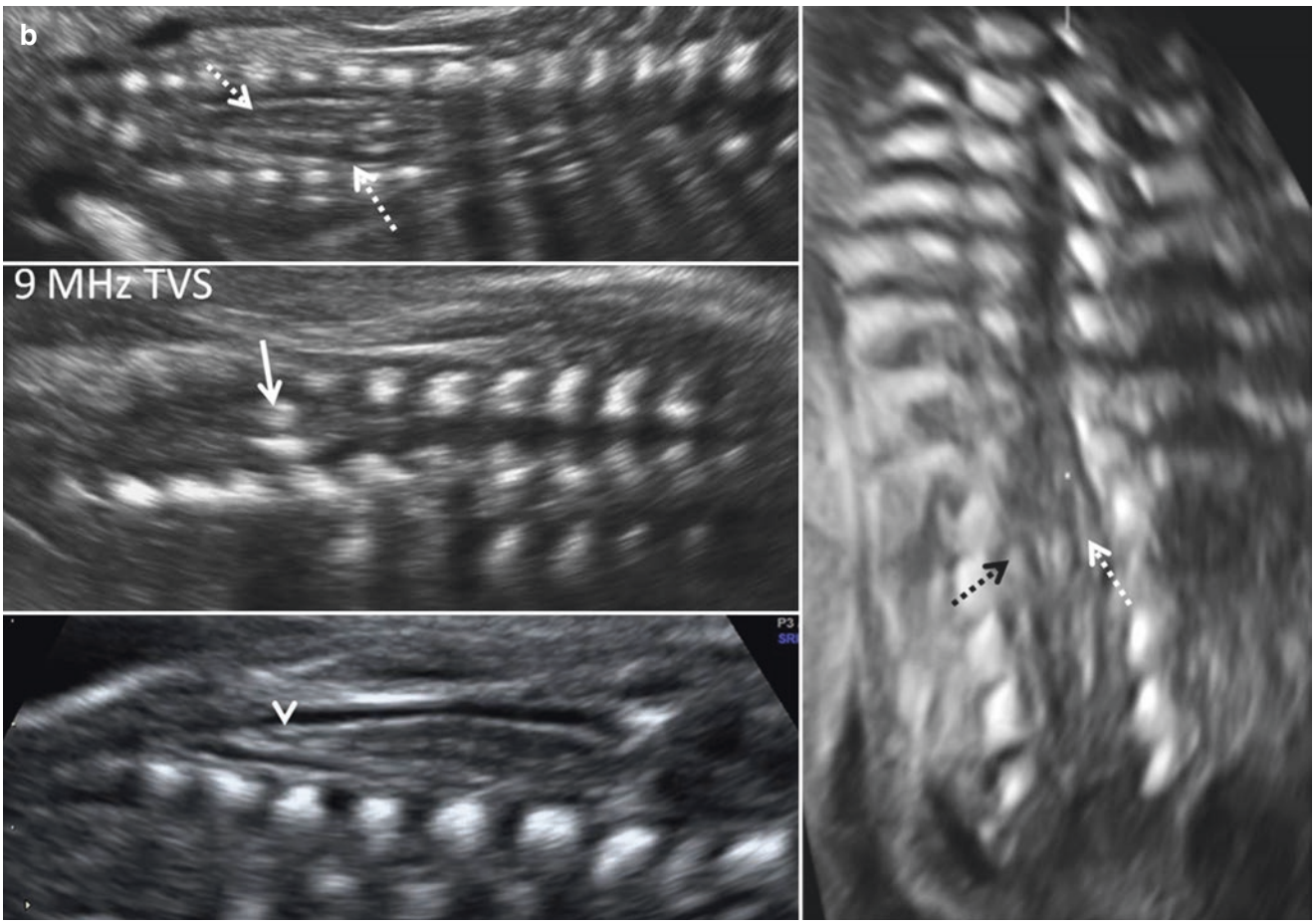

Fig. 6.36 (continued)

7. The cord is often tethered.
8. Associated findings include hemivertebra, kyphoscoliosis, open spina bifida, lipomatous lesions and talipes equinovarus.

6.7.2 Hemivertebra

Failure of chondrogenesis of one lateral half of the vertebral body results in a lateral hemivertebra. Failure of chondrogenesis of the ventral half of the vertebral body results in a dorsal hemivertebra. These result in scoliosis and kyphosis, respectively. Isolated single segment hemivertebra is mostly a sporadic event.

The ultrasound findings are as follows:

1. Asymmetric wedge-shaped vertebral body is seen in the anterior coronal section in a lateral hemivertebra (Figs. 6.37 and 6.38). This finding may not be seen in axial or sagittal sections.
2. In a dorsal hemivertebra, the vertebral body is deficient anteriorly (Fig. 6.39). This is best seen in the sagittal section.
3. The abnormal segment is smaller than the neighbouring normal vertebral segments.
4. One or more segments may be involved. Hemivertebrae most commonly occur in the mid thoracic spine.
5. The spinal deformity may be seen in the first trimester (11–14 weeks). The presence of multiple lateral hemivertebrae on either side may balance the alignment, and scoliosis may not be obvious. Multiple hemivertebrae have a recurrence risk of 5–10%.
6. There is no breach of the skin and subcutaneous layers over the affected segments.
7. 3D coronal-rendered images in the maximum or skeletal mode from sagittal volumes help in the display of the hemivertebra and ascertaining the segmental level (Fig. 6.40).
8. Hemivertebra is a part of VACTERL association. The cardia, kidneys, limbs, upper GI tract and the perianal complex should be studied for associated defects (Figs. 6.37 and 6.40). The autosomal recessive conditions associated with hemivertebra are Jarcho-Levin and Klippel-Feil syndromes.

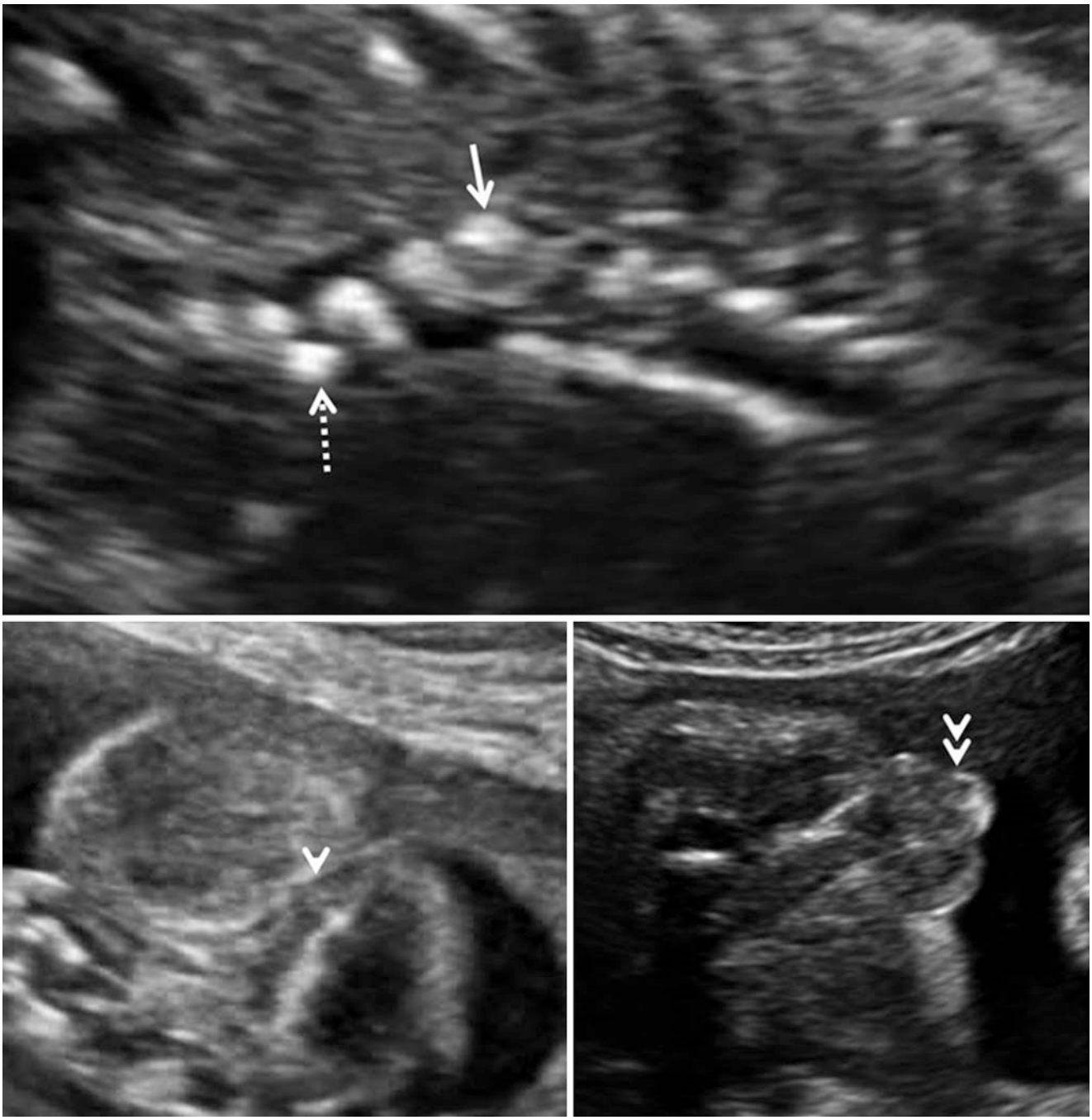

Fig. 6.37 23 weeks (TAS) *L3 and S1 hemivertebra, imperforate anus, penoscrotal hypospadias and single umbilical artery – possible VACTERL association* – coronal section of thoracic spine, axial sections of perineum and external genitalia, lateral hemivertebra at L3 and S1 levels (solid and dotted arrows) with kyphosis, perianal muscular sphincter not seen (arrowhead), penoscrotal hypospadias (double arrowhead)

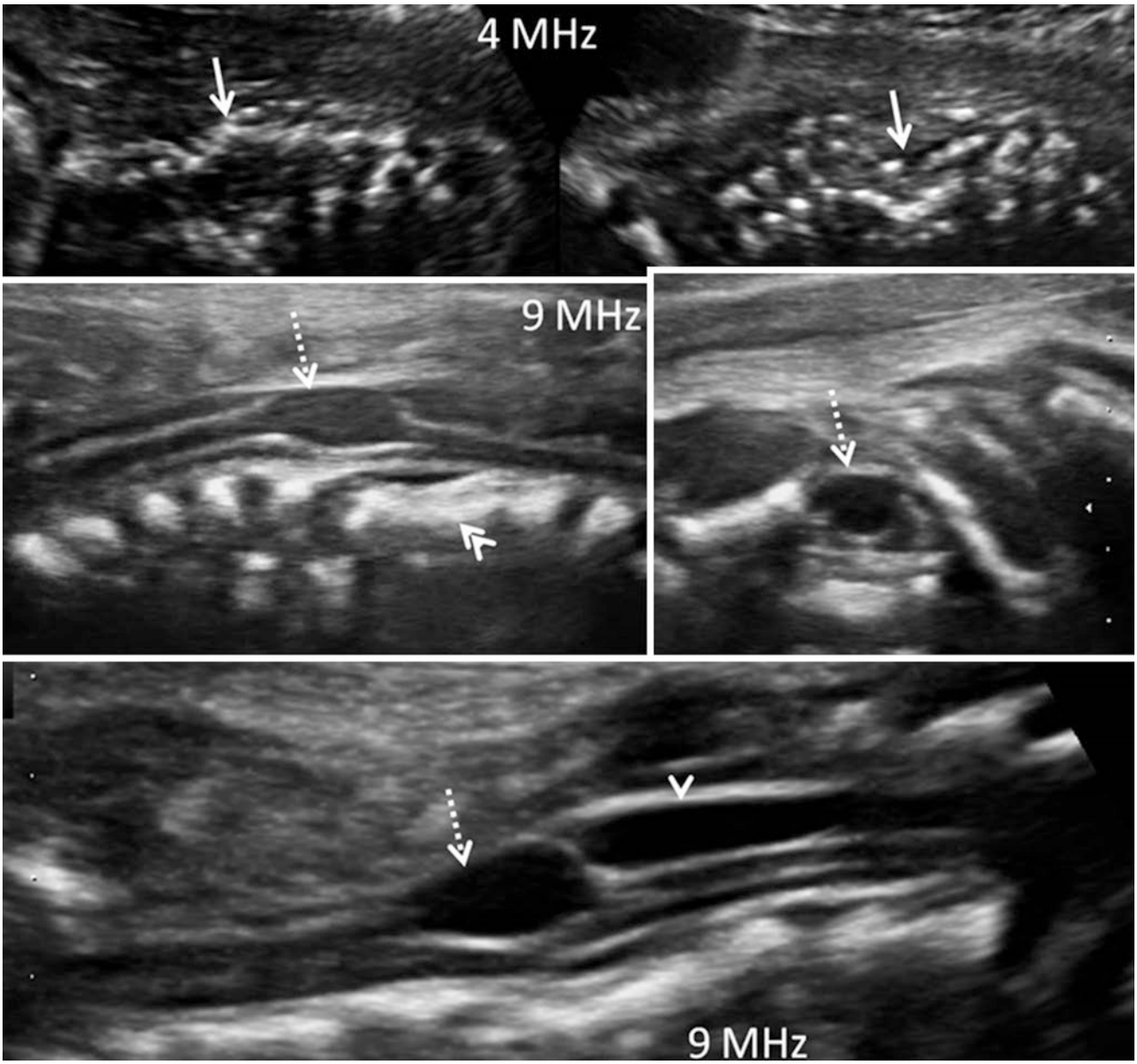

Fig. 6.38 28 weeks (TAS) *multiple cervicothoracic hemivertebra, syringomyelia and possible spinal arachnoid cyst* – coronal, sagittal and axial sections of cervical and upper thoracic spine – irregular cervicothoracic spine due to multiple hemivertebra with kyphosis, widening of the vertebral canal (solid arrows), possible block verterbra (double arrowhead), focal dilatation of the central canal of spinal cord at C7 and T1 level (syringomyelia) (dotted arrow), extra-axial, intradural long cyst dorsal to the spinal cord in the upper thoracic region (arrowhead)

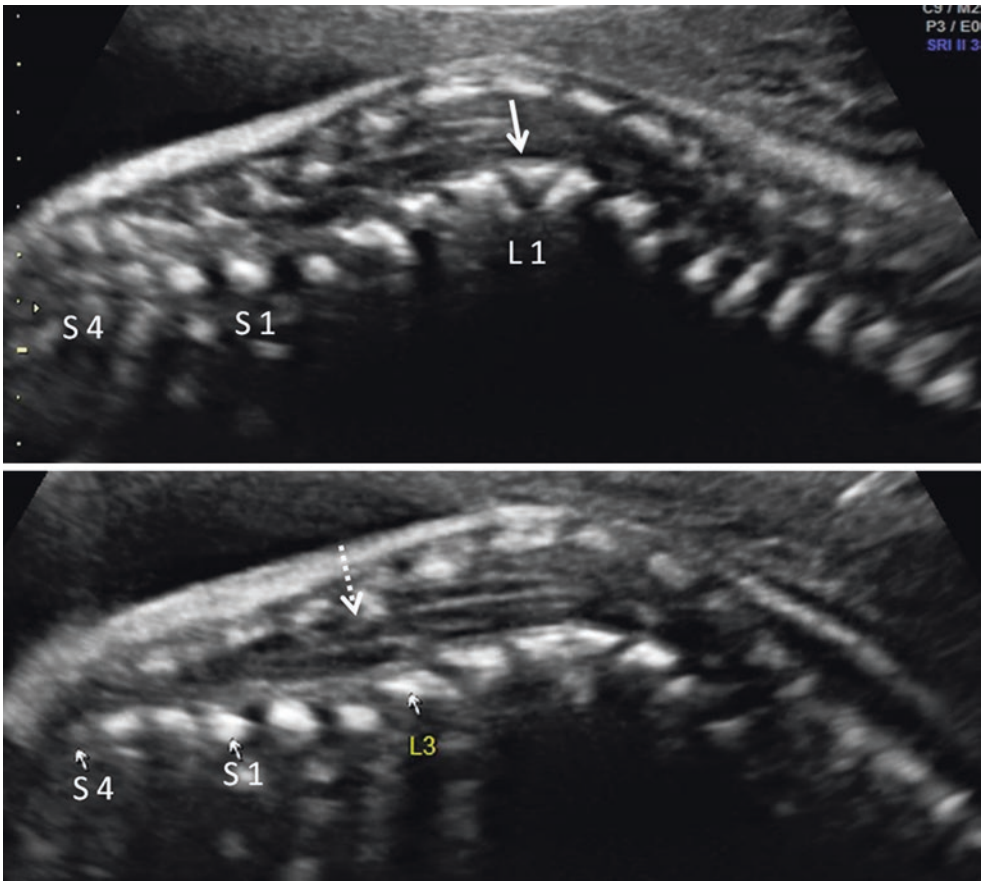

Fig. 6.39 28 weeks (TAS) *dorsal hemivertebra at L1 with angular kyphosis (gibbus) and tethered cord* – sagittal sections of the thoracolumbosacral spine – dorsal wedge-shaped body of L1 as counted from S4 cephalad (solid arrow), conus medullaris is at L4 level indicating tethered cord (dotted arrow)

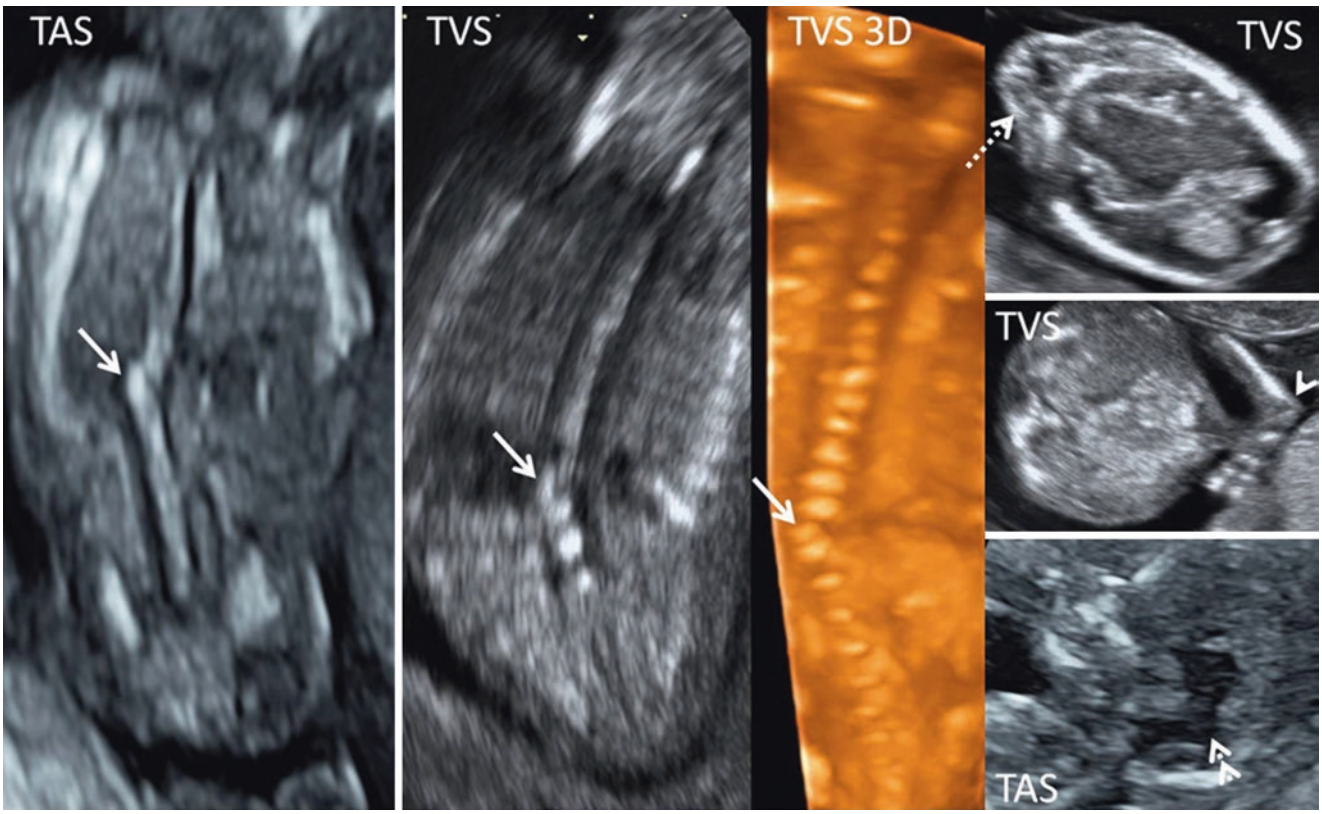

Fig. 6.40 12 weeks (TAS and TVS) *T11 hemivertebra with occipital encephalocele and right clubhand ? VACTERL association* – coronal sections of the spine with 3D rendered image in maximum mode, thalamopeduncular section of cranium, sagittal section of right forearm and hand, intracranial translucency (IT) – T11 lateral hemivertebra with scoliosis (solid arrows), occipital encephalocele (dotted arrow), right clubhand (single arrowhead) and IT abnormality (double arrowheads)

6.7.3 Neurenteric Cyst

Abnormal splitting of the notochord results in non-fusion of the two lateral halves of the vertebral body. This results in a track between the central spinal canal (neuroectoderm) and the gastrointestinal tract (endoderm). An endoderm -lined cyst communicating with the track is seen at the level of the vertebral lesion. This cyst is termed a neurenteric cyst.

1. Hemivertebrae, butterfly vertebrae or block vertebra are seen at the affected level.
2. A cyst is seen anterior to the spine at the level of the vertebral abnormality (Fig. 6.41a, b).
3. Spinal cord abnormality (split cord) may be seen at the affected vertebral level.
4. Concomitant gastrointestinal duplication cysts may be present.

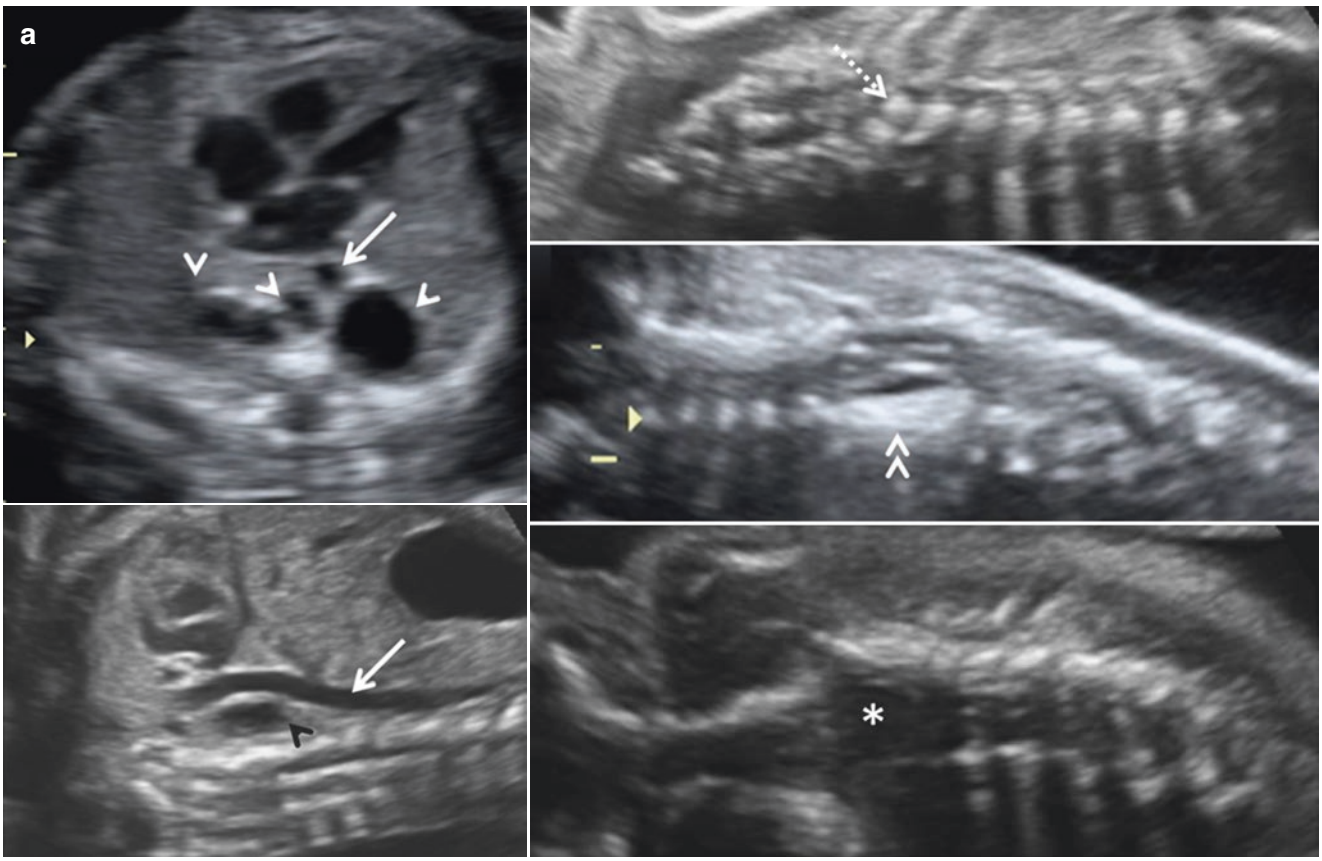

Fig. 6.41 (**a**) 24 weeks (TAS and MRI) *neurenteric cyst* – axial and sagittal sections of thorax, anterior and posterior coronal sections of thoracic spine – retrocardiac, retroaortic, prevertebral tubular folded cystic lesion (arrowheads), descending aorta (solid arrow), hemivertebra (dotted arrow), block vertebra (double arrowhead) and widening of the vertebral canal (*). The spinal findings are at the same level as the posterior mediastinal cystic lesion. (**b**) 24 weeks (TAS and MRI) *neurenteric cyst* – coronal and sagittal sections of thoracic spine, coronal section of chest through the cystic lesion, magnified axial section of thoracic spine – retrocardiac, retroaortic, prevertebral tubular folded cystic lesion (solid arrows), widening of the vertebral canal (dotted arrow) with possible intracanal extension of the cyst (arrowhead), duplicated spinal cord (double arrowhead), coexisting intestinal duplication cyst in the lower abdomen (*). Presence of the spinal defects at the level of the prevertebral cyst confirms neurenteric origin

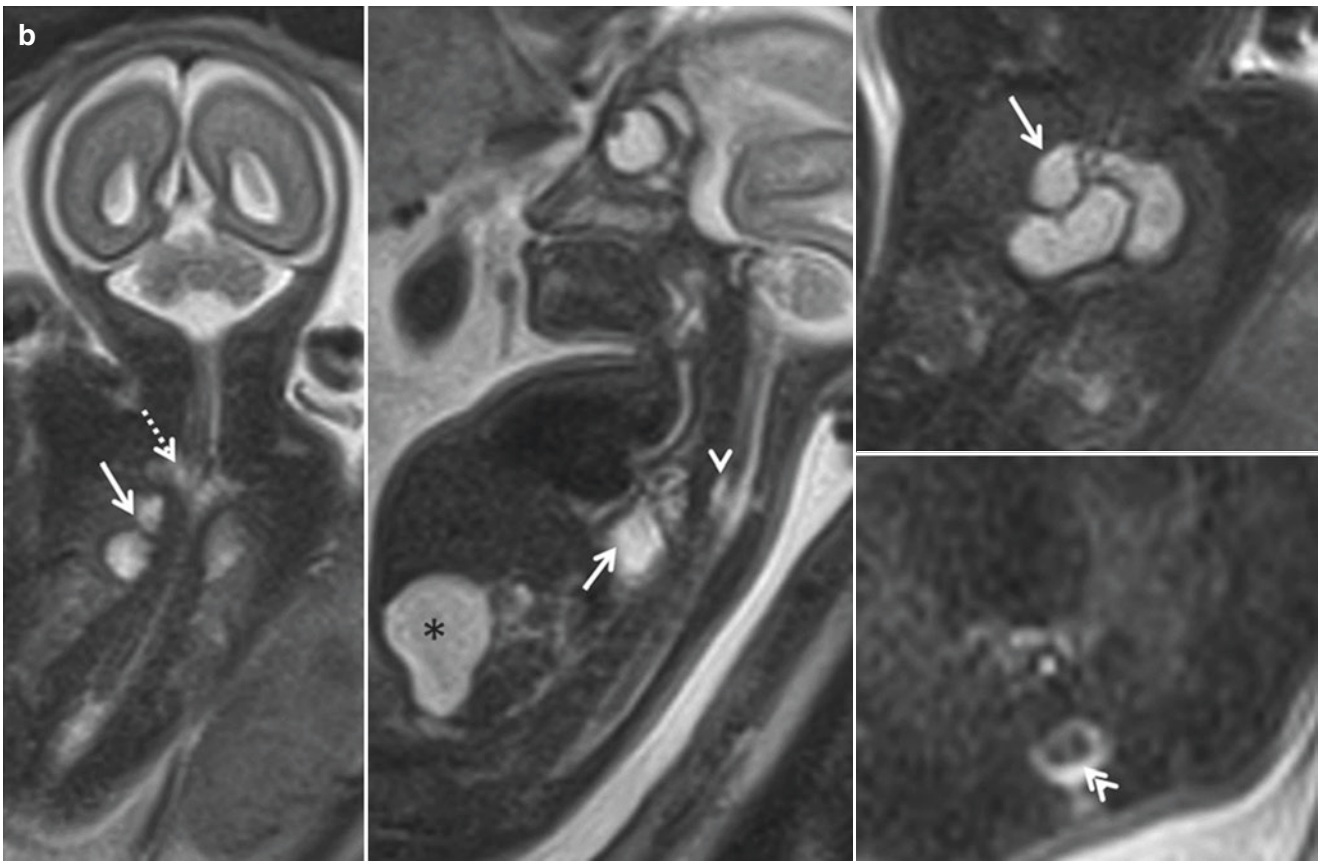

Fig. 6.41 (continued)

6.7.4 Sacral Agenesis

Failure of induction of the caudal neural tube and the surrounding mesodermal structures results in total or partial sacral absence. There is a strong association between maternal diabetes mellitus and sacral agenesis.

1. The sacrum is absent and the last vertebral segment is S1 or higher.
2. The normal sacral taper is absent. Blunt and abrupt ending of the spine is seen.
3. The iliac bones are fused across the midline. The distance between the femoral heads is decreased.
4. Short crown rump length in the 11–14 weeks scan is an early indicator of sacral agenesis in the first trimester.
5. Associated lumbar vertebral absence or abnormalities may be seen.
6. Lower limb neuromuscular sequelae may present as arthrogrypotic changes.
7. Partial sacral agenesis with absence of the one or two terminal segments of the sacrum is more subtle and difficult to diagnose (Fig. 6.42a, b).
8. The kidneys, urinary bladder, genitalia, lower limbs and perianal complex must be assessed.

Sacral agenesis is a part of caudal regression syndrome or sirenomelia sequence (Fig. 6.43).

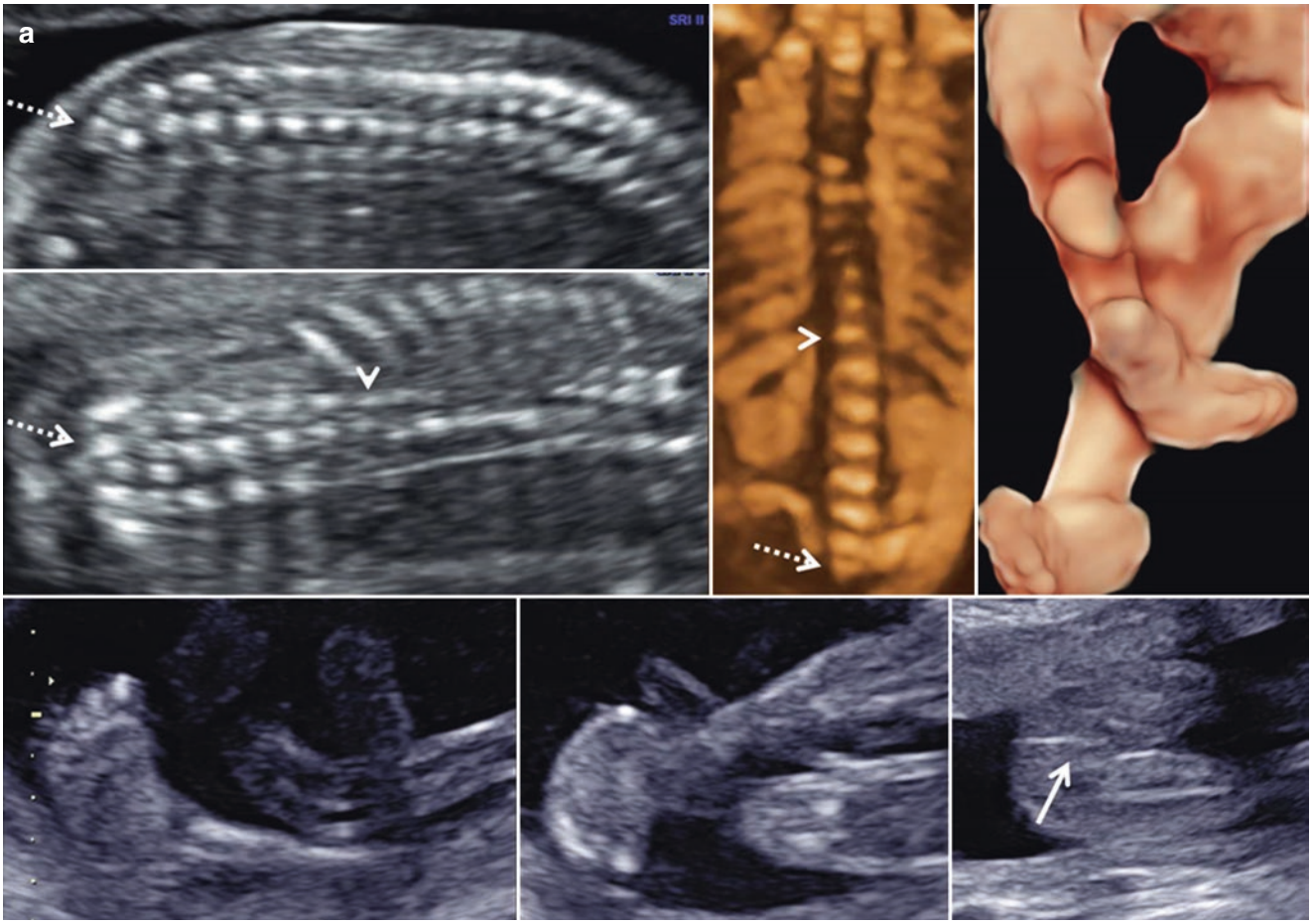

Fig. 6.42 (**a**) 20 weeks (TAS) *partial sacral agenesis with bilateral talipes equinovarus and imperforate anus* – sagittal and coronal sections of thoracolumbosacral spine, 3D rendered coronal view in maximum mode, 3D and 2D rendered views of lower limbs, perineal transverse section – abrupt and truncated sacrum, the sacral taper is not seen, the last segment is S2 (dotted arrows) as counted from T12 caudad (arrowhead), bilateral talipes equinovarus, perianal sphincteric complex is not seen (solid arrow). (**b**) 20 weeks. Prenatal 3D coronal VCI omniview of spine matched with the postnatal X-ray AP spine, abortus with bilateral talipes equinovarus. The truncated sacrum is seen

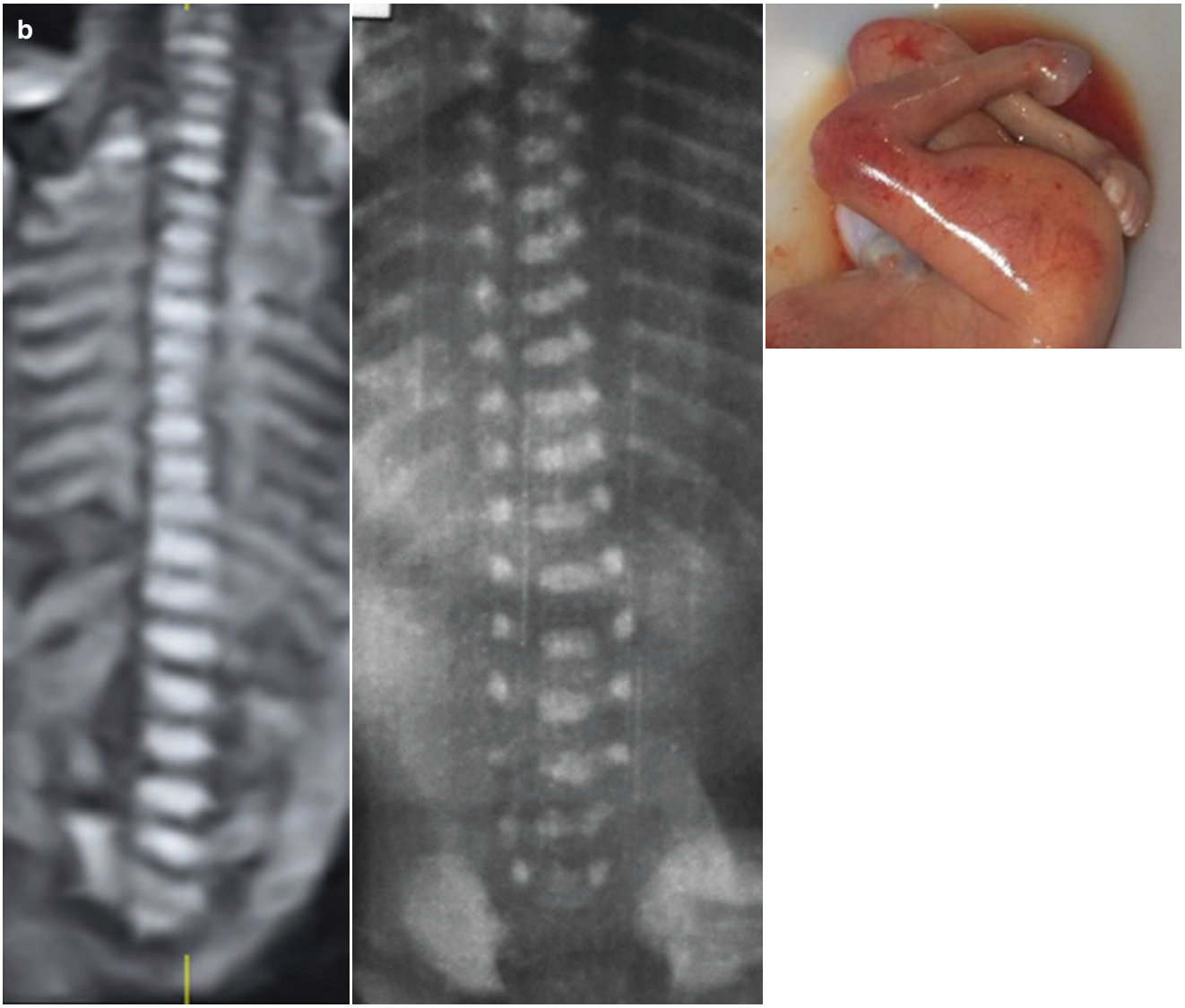

Fig. 6.42 (continued)

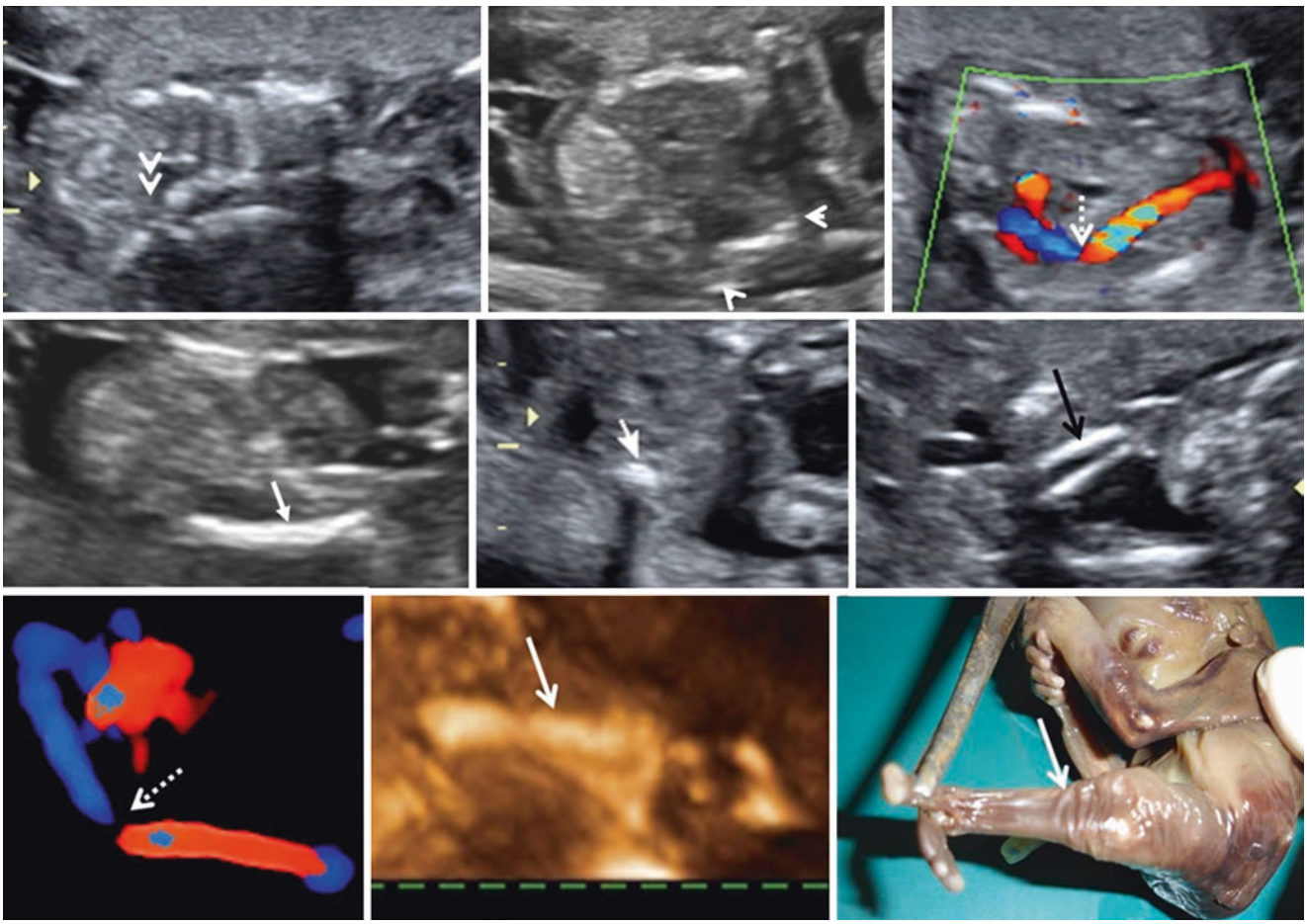

Fig. 6.43 16 weeks (TAS) *sirenomelia sequence* – coronal section of the spine, axial section through the renal fossa, color Doppler of the abdominal aorta, femur longitudinal and axial sections, coronal section of the leg – total sacral agenesis resulting in the truncated spine (double arrowhead), both kidneys are not seen in their anatomical location (arrowheads), the abdominal aorta continues into the persistent vitelline artery in 2D and 3D (dotted arrows), single lower limb noted, single fused femur (solid arrows), fused leg (black solid arrow). Note the anhydramnios as a result of bilateral renal agenesis

Suggested Reading

1. Coleman BG, Langer JE, Horii SC. The diagnostic features of spina bifida: the role of ultrasound. Fetal Diagn Ther. 2015;37:179–96.
2. Ghi T, Pilu G, Falco P, Segata M, Carletti A, Cocchi G, Santini D, Bonasoni P, Tani G, Rizzo N. Prenatal diagnosis of open and closed spina bifida. Ultrasound Obstet Gynecol. 2006;28:899–903.
3. Hoopmann M, Abele H, Yazdi B, Schuhmann MU, Kagan KO. Prenatal evaluation of the position of the fetal conus medullaris. Ultrasound Obstet Gynecol. 2011;38:548–52.
4. Lewis H, Tuite GF, Gonzalez-Gomez I, Baron F, Towbin RB, Towbin AJ, Neville Kucera J. Atretic cephalocele: prenatal and postnatal imaging features. Appl Radiol. 2017;46:36–9.